THE THERMAL-HYDRAULIC CODES COBRA III-C AND TERHID
- AN ANALYSIS AND COMPARISON -

by

Gülsevin ÇAĞIL

B.S. in M.E., I.D.M.M.A.G.S., 1976

Submitted to the Nuclear Engineering Department
in Partial Fulfillment of
the Requirements for the Degree of

MASTER OF SCIENCE
in
NUCLEAR ENGINEERING

Boğaziçi University
1981

APPROVAL OF READERS

This is to certify that I have read and approved the thesis entitled "-AN ANALYSIS AND COMPARISON- OF THERMAL-HYDRAULIC CODES COBRA III-C AND TERHID", submitted by Gülsevin Çağıl in partial fulfillment of the requirements for the degree of MASTER of SCIENCE, Department of Nuclear Engineering, Boğaziçi University.

Doç.Dr.Fahir BORAK
(Thesis Supervisor)

Doç.Dr.Salih DİNÇER

Prof.Dr.Turan B.ENGİNOL

Doç.Dr.Tolga YARMAN

ACKNOWLEDGEMENTS

I would like to express my sincere thanks to my thesis supervisor, Doç.Dr.Fahir BORAK, for his continual guidance and helpful suggestions throughout the whole work.

ÖZET

Bu çalışmada, plâka yakıt elemanlı nükleer reaktör geçici ve sürekli rejim termohidrolik analizi bilgisayar programı TERHİD ve kısmi kanal yaklaşımı ile plâka veya silindirik yakıt elemanlı nükleer reaktörlerin geçici ve sürekli rejim termohidrolik analizi yapan COBRA III-C bilgisayar programlarının analizi ve mukayesesi yapılmıştır.

Her iki programın mukayesesi ve analizi, programlanan ısı iletim ve ısı taşınım modellerini, bu modellerde yapılan kabulleri ve sayısal çözüm yöntemlerini içermektedir.

Sayısal uygulama iki kısımdan oluşmaktadır. Birinci kısımda TERHİD bilgisayar programına uygulanan tek kanal problemi, COBRA III-C programında kullanılarak geçici rejim ara çözümlerinin kendi aralarında çeşitli zaman aralıkları kullanarak mukayesesi yapılmıştır.

İkinci kısımda ise geçici rejim analizinde, soğutucu giriş sıcaklığı ile miktarında ve güç üretiminde zamana bağlı değişimlerin etkileri, ayrı ayrı basamak değişimi olarak aynı problemi her iki programa uygulayarak incelenmiştir.

ABSTRACT

In this work the thermal-hydraulic programmes TERHİD, which makes steady state and transient thermal-hydraulic analysis for plate type nuclear fuel elements, and COBRA III-C, a computer programme for steady state and transient state thermal-hydraulic analysis of rod bundle fuel elements with subchannel approach analysed and compared.

The comparison of the two programmes cover the analysis of the conduction and the convection models, the assumptions made in the models, and the solution algorithms.

The numerical applications consist of two parts. In the first part the sample problem given in TERHID is applied as input to COBRA III-C. The transient solutions for different time increments are intercompared for this programme. In the second part another application is carried out for the identical problem using both codes by considering the effect of the inlet temperature change, inlet mass flux change and power change as a function of time during transients.

CONTENTS

LIST OF TABLES

LIST OF FIGURES

NOMENCLATURE

A_i	Cross-sectional area (ft^2), (m^2)
C_1, C_2	Integration constants (TERHID)
c	specific heat of the element (Btu/lb.^oF)
c_1	specific heat of the fuel (J/kg ^oC)
c_2	specific heat of the cladding (J/kg ^oC)
c_{ij}	thermal conduction coefficient (Btu/hr.ft. ^oF)
D	hydraulic diameter (ft)
D_e	Equivalent diameter (m)
Dr	rod diameter (ft)
d_1, d_2	Integration constants (TERHID)
F_i	frictional losses per unit length (N/m)
f	friction factor (dimens-onless) (COBRA)
f_T	turbulent momentum factor (COBRA)
g_c	gravitational constant (COBRA)
h	heat transfer coefficient (Btu/hr.ft^2.^oF)
h	convective heat transfer coefficient (W/m^2.^oC)
h_1,h_2	equivalent heat transfer coefficient (W/m^2.^oC)
h_i	enthalpy of the coolant (J/kg), (Btu/lb_m)
$\overline{h_i}$	enthalpy from the previous time (J/kg)
h*	enthalpy carried by diversion crossflow (Btu/lb_m)
k	thermal conductivity (Btu/hr.ft.^oF)
k_1	fuel thermal conductivity (W/m^oC)
k_2	cladding thermal conductivity (W/m^oC)
K_i	spacer loss coefficient
L	channel length (ft)
L_1	fuel thickness (m)
L_2	cladding thickness (m)
m	Flow rate (lb/sec)
m_i	Flow rate (kg/sn)
$\overline{m_i}$	Flow rate at the previous time (kg/sn)
O_i	differential operator i=1,2,3,4
P	Reactor power (W)

P, p_i, p_j	pressure (lb_f/in^2)
p_i	pressure (N/m^2)
p_r	Prandl number (dimensionless)
$q(j,k)$	power production in fuel element (j,k)
q'_i	power transfered from fuel to coolant per unit length. (W/m)
q'	heat addition per unit length (Btu/hr.ft)
q''	heat flux (W/m^2)
$\bar{q}''$	average heat flux ($Btu/hr.ft^2$)
q'''	volumetric power (W/m^3)
q'''	power density ($Btu/hr.ft^3$)
r_1, r_2	roots obtained from the differential equations eq. (B.26)
Re	Reynolds number (dimensionless)
s	plate, (rod) spacing (ft)
$\bar{\rho}$	density of the element (lb/ft^3)
ρ_i	density of the coolant (kg/m^3)
ρ_1	fuel density (kg/m^3)
ρ_2	cladding density (kg/m^3)
$\bar{\rho}_i$	coolant density at the previous time (kg/m^3)
T_i	Temperature (^oF)
$\bar{T}_i$	Temperature at the previous time (^oF)
T_1	Fuel temperature (^oC)
$\bar{T}_1$	Fuel temperature at the previous time (^oC)
T_2	Claddin temperature (^oC)
$\bar{T}_2$	Cladding temperature at the previous time (^oC)
T_{12}	Fuel-cladding interface temperature (^oC)
T_f	Temperature of the coolant (^oC), (^oF)
t	Time (sec.)
t_{clad}	cladding thickness (ft)
U_i	Internal energy of the coolant (Btu/lb) (J/kg)
U	Effective momentum velocity (ft/sec.)
U''	Effective enthalpy transport velocity (ft./sec.)
U^*	Effective velocity carried by diversion crossflow (ft/sec.)
V	Liquid specific volume (ft^3/lb)
V'	Effective specific volume for momentum ($ft^3./lb$)

V_i	Coolant velocity (m/sec)
$\bar{V}_i$	Coolant velocity at the previous time (m/sec.)
W	Diversion crossflow between adjacent subchannels (lb/sec.ft.)
W'	Turbulent crossflow between adjacent subchannels (lb/sec.ft)
α_1, α_2, α_3	heat transfer coefficients, H_1, h_2, divided by density, specific heat and length.
β	mixing parameter (dimensionless)
θ	Channel orientation with respect to vertical (Radions)
ϕ_i	Friction multiplier (dimensionless)

COBRA III-C uses English Engineering system of units

CHAPTER I
INTRODUCTION

a) Background

The economically recoverable fossil fuel resources of coal, oil, and natural gas are finite, while hydro-power have a limited exploitation potential. Available fossil fuel reserves of the world will not be sufficient to supply the huge energy demand in the future. Also some of the fossil fuels are very valuable for other purposes like chemical industry, heavy industry, transopratiton, heat production, etc.

It is very important to develop new sources of energy production and to produce a constant replacement of classical resources by new ones. Therefore, nuclear energy, produced by fissionable materials, is a very attractive alternative today and since late sixties it is economically feasible in many regions of the world.

The demand for electric energy consumption is increasing much faster then the total energy production, and due tc the preference for conversion into electricity and subtantial reduction in air pollution, the role of nuclear energy is expected to gain importance with time (Aybers.N.-1970)(Searby.P.J.-1969).

It is expected that, during the next decade world's nuclear generating capacity will increase from 31.000 MW(e) in 1970 to about 325000 MW(e) in 1985. This amount will be about one-eight of the world's electricity generating capacity.

In addition to the power reactors producing useful energy there are many research reactors at low-power levels and material testing reactors etc.

In the design of all reactor types, the process of heat generation within the reactor fuel element and the heat transport from the fuel element, and the thermal tarnsport parameters in various operating conditions play an important role. The term various operating conditions include the steady state analysis for a given power level; transient analysis with the change of power, inlet coolant temperature, inlet mass flux, as a function of time, and also includes the effect of accident possibility. Therefore the thermal-hydraulic analysis are closely associated with safety considerations. For example; in water reactors a loss-of-coolant accident can lead to a decrease in heat, removal capacity of the primary coolant system as it vaporizes during blowdown.

Generally in a typical system the thermal-transport path proceeds from a point of fission energy deposition within the fuel, through layers of the fuel, through the cladding-coolant interface. The heat is then transported into the body of the flowing fluid (coolant). This causes a rise in the temperature of the coolant. The coolant transports the absorbed energy to the heat exchanger, in which steam is generated and the steam is then led to the turbine to produce electricity. However in some research reactors the energy of the secondary cooling system is not converted into electricity, the secondary cooling system is used to cool the primary system and the core.

As mentioned above, the energy released by fission takes place within the fuel element, and the generated heat must be transported through the fuel element to the heat transfer medium, without producing temperatures that could

cause failures of the fuel. The word failure in this sense means a change in physical properties or dimensions, as well as melting or corrosion. In a general sense therefore failure is a loss in the functional abilities of the fuel element.

The thermal design of a fuel element must meet certain criteria; (Sesonske - 1973).

- Maximum temperatures must not lead to deteriorations of the fuel material, such as change in physical properties or in dimension of the fuel materials, or lead to melting, corrosion, etc.

- Stresses due to the effects of thermal gradients and accumulated fission gases should lie within the limitations and must not lead to the possibility creep or embrittlement of the cladding.

- The thermal flux must be below the critical heat flux, which causes a marked decrease in heat transfer coefficient resulting in an increase of the fuel element temperature at constant heat generation rate. The thermal design of a fuel element is therefore concerned with the effect of temperature and thermal transport on the fuel element.

Therefore from the point of possibility of fuel rod damages, and from the point of safety of a nuclear power plant, the thermal hydraulic analysis is the most important and the most complex part of the reactor design.

The complexity is due to the spatial variations, physical properties of the fuel material, fuel rod dimensions, during transient state, economics, and neutronic parameters depending on temperature, evaluations of normal and abnormal transient conditions. Therefore this detailed, complex, and

time requiring analysis can be made by using thermal-hydraulic computer codes.

The reactor thermal-hydraulic programmes can be classified into a few catagories . Some programmes include a solution of neutron-diffusion equations or neutron-transport equations and perhaps kinetic equations in addition to an analysis of fuel-element thermal-transport and channel hydraulics. Other programmes are limited to a detailed steady state and transient thermal-hydraulic calculations of the reactor core including primarly and secondary coolant systems. Each type has it's use.

As examples of the thermal-hydraulic codes, the fo-lowing programmes can be mentioned (Weisman, Bowring - 1975)(C.P.A.-ANL.).

CAT-II, makes transient analysis, based on an open channel model, without considering the crossflow resistance.

COBRA III-C; steady state and transient thermal-hydraulic programme of rod bundle and plate type fuel elements.

HAMBO; makes subchannel analysis of rod bundles.

MIXER; THINC, make subchannel analysis of rod bundles.

TERHID; steady state and transient thermal-hydraulic analysis of water cooled plate type fuel elements. For some of the codes only limited information is available in the literatures. The hydraulic model for most of these thermal-hydraulic programmes are almost the same but they differ from each other in the solution method and in the input information requirement especially for operating conditions.

b) Scope

There are two thermal-hydraulic programmes operational at Boğaziçi University, namely TERHİD (Borak-79) and COBRA III-C (Rowe-73).

TERHID performs the thermal-hydraulic analysis for steady state and transient state of water-cooled reactors with plate type fuel elements.

COBRA III-C performes the steady state and transient thermal-hydraulic analysis of rod bundle and plate type fuel elements.

The object of this thesis is to analyse the mathematical modelling and assumptions used in the codes, the solution algoritm of the two programmes and to compare numerical solutions for identical transient problems in order to determine whether consistent set of results are obtained, and to obtain the effect of the assumptions on the numerical values in the numerical analysis.

CHAPTER-II

CONDUCTION MODEL OF THE CODES

The purpose of this chapter is to discuss the conduction model, which forms a part of the mathematical model of the codes developed for nuclear thermal-hydraulic analysis during both steady state and transient conditions.

The first part, of this chapter includes a general description of the conduction models of the codes COBRA III-C (Rowe-71) and TERHİD (Borak-79) and in the second part the conduction models of two codes will be compared and a summury will be made.

II-A. BASIC ASSUMPTIONS AND GENERAL DESCRIPTION OF THE CONDUCTION MODELS

The fuel rod heat transfer model of COBRA III-C (Rowe) allows calculation of fuel and cladding temperatures during steady state and transients by specifying power density.

For fuel and cladding temperature calculations the fuel rod heat transfer model included in COBRA III-C considers radial conduction within the fuel by dividing the fuel into equally spaced radial nodes and plus a node for the cladding. In treating the problems of heat removal from the fuel element, as a simplifying assumption axial and circumferential heat conduction are ignored. Axial heat conduction can be ignored because axial temperature gradients are usually small

compared to the radial temperature gradients. The circumferential heat conduction is neglected to maintain a reasonable limit on the number of fuel nodes. This last assumption is acceptible particularly if the heat transfer coefficients and fluid temperatures are rather uniform around the fuel rod.

The numerical solution of conduction model of COBRA III-C uses an implicit finite difference scheme that is stable for all time steps. The equations used for the numerical solution of COBRA III-C are given in subchapter II-B-i and derivation of equations for conduction model are given in App. A.

The fuel heat transfer model included in TERHİD considers plate type fuel elements and allows the calculation of the fuel and cladding temperatures by specified power. The fuel and cladding temperatures are calculated by using lumped parameter technique and assuming one dimensional heat transfer, so thus the thickness of the plate must be small compared with other dimensions.

The heat transfer coefficients at fuel-cladding and cladding-coolant interfaces are evaluated by considering steady state conditions. For the numerical solutions in conduction model TERHİD uses equations of heat conduction given in subchapter II-B-ii and derivation of fuel heat transfer equations are given in App. B.

II-B. MATHEMATICAL MODEL OF CONDUCTION

II-B-i. CONDUCTION MODEL IN COBRA III-C

The time dependent general conduction equation (Wakil-71)

with heat generation in cylindrical coordinates by making the assumptions that axial and circumferential heat conduction is negligible;

$$\rho c \frac{\partial T}{\partial t} = k\left[\frac{\partial^2 T}{\partial r^2} + \frac{1}{1}\frac{\partial T}{\partial r}\right] + q''' \qquad (2.1)$$

where ρ, c, k, T, r, q''' are density (lb/ft^3), specific heat ($Btu/lb.^oF$) thermal conductivity ($Btu/hr.ft^oF$), temperature (^oF) and radius of the fuel rod for plate type r is taken to be equal to the plate thickness (inc.) and volumetric thermal source strength ($Btu/hr.ft^3$) respectively.

From equation (2.1) the heat transfer equations for the fuel are written in finite difference form (App. A) as;

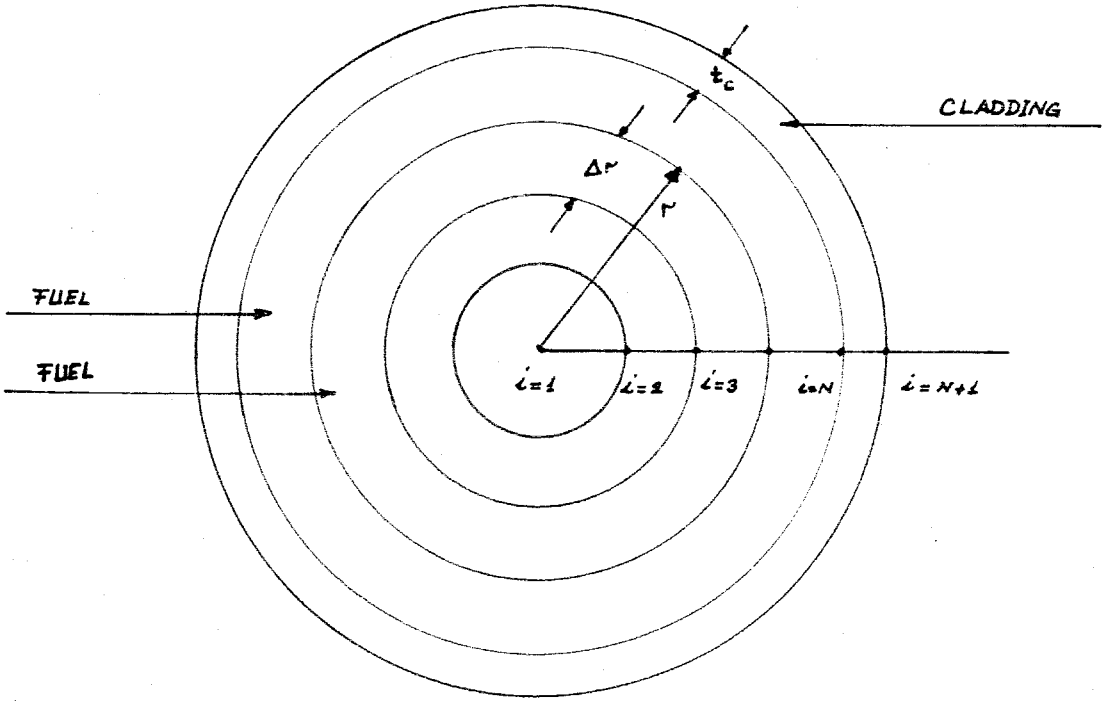

FIGURE II-1- Fuel Model Node Designation with concentrig rings.

The temperature at fuel center:

$$\rho c \frac{T_1}{\Delta t} + q_1''' = T_1 \left[\frac{\rho c}{\Delta t} + \frac{4k}{\Delta r^2}\right] - \left[\frac{4k}{\Delta r^2}\right] T_2 \qquad (2.2)$$

where subscrip (1) denotes the fuel center designated in Figure (II-1) and the overscore bar ($\bar{}$) denotes previous time.

The temperature in fuel region:

$$\rho c \frac{\bar{T}_i}{\Delta t} + q_i''' = \left[\rho c \frac{1}{\Delta t} + \frac{2k}{\Delta r^2}\right] T_i - \left[\frac{k}{\Delta r^2} + \frac{}{2\Delta r^2(i-1)}\right] T_{i+1}$$

$$+ \left[\frac{k}{2\Delta r^2(i-1)} - \frac{k}{\Delta r^2}\right] T_{i-1} \qquad (2.3)$$

For fuel temperature at fuel-cladding interface.

$$\rho c \frac{\bar{T}_N}{\Delta t} + q_N''' = \left[\frac{2k}{\Delta r^2} - \frac{c}{t} - \frac{k \cdot hgap}{\Delta r(N-1)}\right] T_N - \frac{2k}{\Delta r^2} T_{N-1}$$

$$\frac{k \cdot hgap}{\Delta r(N-1)} T_{N+1} \qquad (2.4)$$

where the locations i and N+1, N, N-1, are designated in Figure (II-1) and hgap is the gap conductance (Btu/hrft^2 ^oF) To combine the conductance of the cladding and the gap, at the fuel-cladding interface hgap is taken as an effective heat transfer coefficient (App. A) for the cladding temperature:

$$(\rho c)_{clad} \frac{\bar{T}_{N+1}}{t} + q'''_{N+1} = \left[\frac{h_{surf}}{t_{clad}} + \frac{h_{gap}}{t_{clad}} \frac{T_N}{r_{N\ 1}} - \frac{(\rho c)_{clad}}{t}\right] T_{N+1}$$

$$- \frac{h_{surf}}{t_{clad}} T_f - \frac{h_{gap}}{t_{clad}} \frac{r_N}{r_{N+1}} . T_N \quad (2.5)$$

Where h_{surf} denotes surface heat transfer coefficient and T_f is the fluid temperature.

II-B-ii. CONDUCTION MODEL IN TERHİD

The unsteady state temperature problem of the fuel and the cladding are formulated and solved by using lumped parameter technique (Wakil, Arpacı-66) and assuming one dimensional heat transfer in fuel and cladding. For the fuel, the heat balance equation (Borak-79) is given as; Figure (II-2)

$$\rho_1 c_1 L_1 y dz \frac{dT_1(t)}{dt} = q''' y . dz . L_1 - q''.ydz \quad (2.6)$$

Where; ρ_1, c_1, L_1, T_1, q''', and q'' are fuel density (kg/m^3), fuel specific heat (J/kg^oC), fuel half thickness (m), fuel temperature (^oC), power density (W/m^3) and heat flux (W/m^2) respectively.

The left side of equation (2.6) gives the accumulation of heat and the right side indicates heat generation in the fuel minus the heat conducted through the fuel to the cladding.

Equation (2.6) can be written as;

$$\frac{dT_1(t)}{dt} + \alpha_1 T_1(t) - \alpha_1 T_2(t) = \frac{q'''}{\rho_1 c_1} \quad (2.7)$$

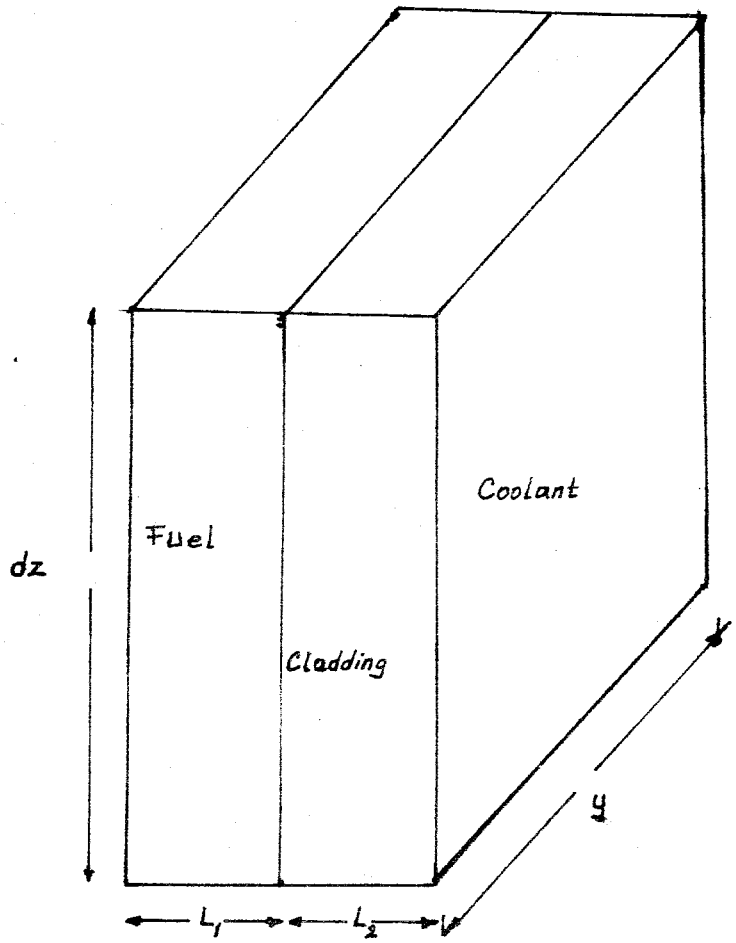

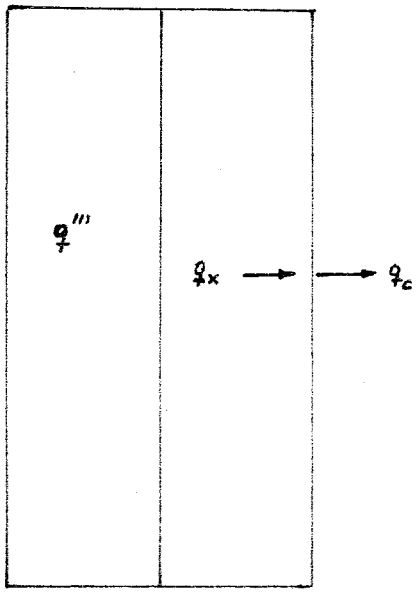

FIGURE II-2- Fuel and Cladding Design of TERHİD.

Where;

$$\alpha_1 = \frac{h_1}{\rho_1 c_1 L_1}$$

As written for the fuel, the heat balance equation for the cladding is;

$$\rho_2 c_2 L_2 y\, dz \frac{dT_2(t)}{dt} = h_1\left[T_1(t) - T_2(t)\right] ydz - h_2\left[T_2(t) - T_f\right] \qquad (2.8)$$

Where; ρ_2, c_2, L_2, $T_2(t)$, T_f, h_1, h_2 in equation (2.8) are cladding density (kg/m^3), cladding specific heat (J/kg^oC), cladding thickness (m), cladding temperature (^oC), fluid temperature (^oC), heat transfer coefficient from the fuel to the cladding, and from the cladding to the coolant ($W/m^2\ ^oC$). These coefficients are taken as equivalent heat transfer coefficients.

Equation (2.8) can be written as;

$$-\alpha_2\ T_1(t) + \frac{dT_2(t)}{dt} + \alpha_3\ T_2(t) = (\alpha_3 - \alpha_2)\ T_f \qquad (2.9)$$

Where:

$$\alpha_2 = \frac{h_1}{\rho_2 c_2 L_2} \qquad \text{and} \qquad \alpha_3 = \frac{h_1 + h_2}{\rho_2 c_2 L_2}$$

Equation (2.7) and (2.9) are coupled differential equations and can be solved for $T_1(t)$ and $T_2(t)$ (Appendix B).

The fuel temperature is calculated from;

$$T_1(t) = C_1\ e^{r_1 t} + C_2\ e^{r_2 t} + \alpha_3 \beta + T_f \qquad (2.10)$$

Where

C_1 and C_2 are constants (are given in Appendix B) and the cladding temperature:

$$T_2(t) = C_1 \frac{(r_1+r_2)}{\alpha_1} e^{r_1 t} + C_2 \frac{(r_2+r_1)}{\alpha_1} e^{r_2 \cdot t} + \alpha_2 \beta + T_f \qquad (2.11)$$

where

$$\beta = \frac{q''' / \rho_1 c_1}{\alpha_1(\alpha_3 - \alpha_2)} \qquad \text{(App. B)}$$

The equivalent heat transfer coefficients are derived by assuming steady state temperature distribution in fuel and cladding (App. B);

$$h_1 = \frac{1}{\frac{L_1}{3k_1} + \frac{L_2}{2k_2}} \qquad (2.12)$$

$$h_2 = \frac{1}{\frac{1}{h} + \frac{L_2}{2k_2}} \qquad (2.13)$$

Where h denotes the convective heat transfere coefficient.

II-B-iii. SUMMARY AND COMPARISON OF CONDUCTION MODEL OF THE CODES

In this chapter the conduction models of COBRA III-C, and TERHİD are descriped. Two codes do not have the same conduction model. They differ from eachother by the formula-

tion. COBRA III-C calculates the fuel center temperature from equation, (2.2) temperature in fuel region from (2.3) cladding temperature from (2.5) and the temperature at fuel cladding interface from (2.4) by using an implicit finite difference sheme for plate type and cyclindrical fuel element (App. A).

An effective gap conductance coefficient is used at fuel-cladding interface. The surface heat transfer coefficient is arbitrarily specified through heat transfer correlations.

The set of equations given in section II-B-i are arranged into a tridiagonal system of equations and solved by using Gauss elimination method. The same set of equations are used for the plate type fuel element except the radial coordinate term $|1/r \frac{\partial T}{\partial r}|$ (App. A) used for the cyclindrical fuel element.

In TERHID the fuel temperatures, and cladding temperatures are calculated from equations (2.10) and (2.11) and the constants used in the equations are found from (B.26), B(40) and (B41) only for the plate type fuel element, with the use of the lumped parameter approach. For the fuel and cladding temperature calculations, equivalent heat transfer coefficients are used by assuming the formes for steady state temperature distribution within the fuel and the cladding. The cladding temperature is calculated by ignoring the gap conductance.

The surface heat transfer coefficient is specified through heat transfer correlations (App. E).

TERHID requires the reactor power and performes the calculations of the power produced at each plate or power

produced at each plate can be supplied as input, this may supply a more accurate result for the transient analysis, but COBRA-III-C requires the heat flux and the power density is defined in terms of the equivalent impressed flux by neglecting the capacitance of the fuel element.

These form the main difference between the codes for conduction model.

CHAPTER-III

CONVECTION MODEL OF THE CODES

In this chapter the convection models of the codes, COBRA III-C and TERHİD will be discussed. The first part consists of a general description of the convection models used in the codes. The second part includes the conservation equations of mass, energy and momentum forming the foundation of the convection model. And the third part gives a summary and comparison of the models.

III-A. BASIC ASSUMPTION AND GENERAL DESCRIPTION OF THE CONVECTION MODELS

The convection model included in COBRA III-C considers subchannel analysis. In this technique the rod cluster, cooled by a fluid passing axially along the rods, is considered to be subdivided into a number of parallel interacting flow subchannels between the rods. The equations of mass, energy, and momentum conservation are solved to give the radial and axial variations in fluid enthalpy and mass velocity. The interactions between subchannels form the important part of the physical model.

This interaction is divided into two processes, i.e., crossflow and turbulent mixing. The crossflow consists of mass transfer between subchannels, in the presence of a radial pressure gradient and the turbulent mixing consists of a

mixing process independent of the pressure gradient, but due to the turbulent nature of the flow.

a) Basic principles of subchannel analysis;

The cross-sectional areas of subchannels are usually defined by lines joining the rod centers (Figure 3-1).

The analysis is made by dividing the channel length into a number of smaller intervals for calculation purposes. The set of simultaneous differential equations of mass, energy and momentum conservation are written in finite difference form and solved iteratively, taking into account crossflow and turbulent mixing, to give a map of the massflow and enthalpy at each mesh point in the cluster.

The general simplication in the subchannel analysis is made by neglecting the flow and enthalpy gradients in the subchannels, and assuming that there is only flow and enthalpy gradients across the subchannel boundaries, so in a sense this is also a lumped approach.

b) Cross flow;

The magnitude of cross flow is much smaller than that of axial flow. It's effect on the axial flow is negligible, at least under normal treactor operation. Even under abnormal operation conditions, where a few flow passages are blocked, the induced perturbation on the axial flow will be small. This small crossflow however, could have a noticeable influence on the thermal fied.

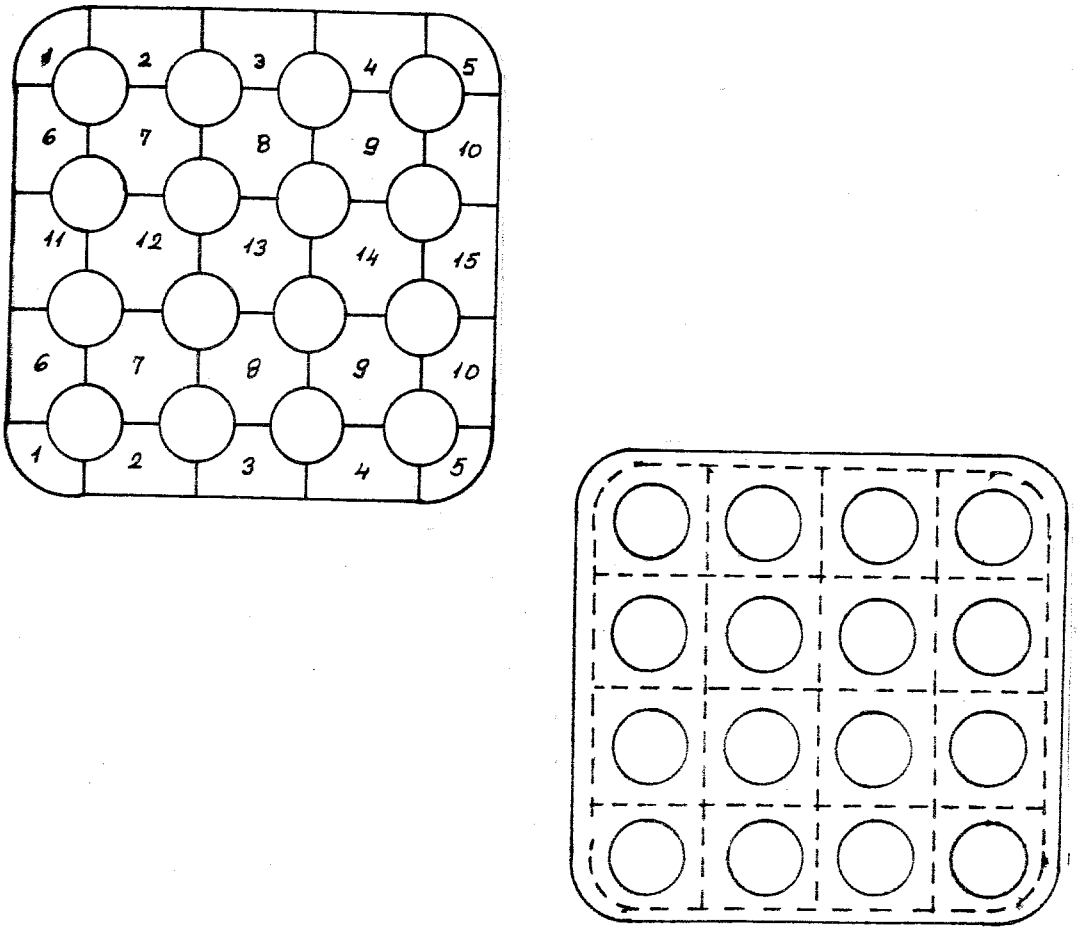

FIGURE (3-1)- Subchannel Area.

c) Turbulent Mixing;

Turbulent mixing plays an important role in equalizing the temperature differences of the coolant, across and within a fuel rod bundle. Therefore the selection of an accurate mixing coefficient is crucial in correctly predicting the thermal-hydraulic behaviour of fuel-rod bundle flow. This selection depends on roughened and smooth surfaces, and the affect of roughness on turbulent mixing is still an open question .(Eckert,Irvine-69),(Donne,M.D.,-73),(Sesonske.-73), (C.Cazley., et.al.,-71).

On the other hand according to the studies , it is known that the turbulent mixing depends strongly on the geometrical arrangement of the fuel pins between two adjacent subchannels and is relatively sensitive to the rod spacing - effective centroid length ratio. When this ratio is reduced, the turbulent interchange decreases due to the possible relaminarization of the flow between the narrow gap of two fuel pins. This is expected by its physical intuition that w'_{ij} (turbulent crossflow between adjacent subchannels i, j) must be zero as the ratio rod spacing - effective centroid length goes to zero.(C.Gazley., et al.,-71).

Using subchannel approach and by making suitable assumptions concerning the flow and crossflow in the subchannels and between the subchannels the equations involved in the convection model of COBRA III-C are written for each subchannel.

The basic assumptions are given below:

Each subchannel contains one dimensional, two phase, seperated slip flow including turbulent crossflow and diversion crossflow as a result of flow redistribution between adjacent subchannels. It is assumed that the turbulent crossflow existing between adjacent subchannels causes no net flow redistribution. Sonic velocity propagation effects are ignored. The diversion crossflow velocity is small compared to the axial velocity within a subchannel.

The convection model of TERHİD is simpler than the convection model of the programme COBRA III-C. Basically the conservation equations of mass, energy and momentum are

similar except the terms existing due to the subchannels in COBRA III-C. TERHID performs single channel thermal-hydraulic analysis, and also assumes single phase flow within the channel. The equations in convection model of TERHID are solved to give the axial variations in fluid enthalpy and pressure differences along the channel.

The system considered by TERHID where it is applicable, provides more simple and more economical and rapid solutions to the single channel thermal hydraulic analysis.

III-B. MATHEMATICAL MODEL OF CONVECTION

III-B-i. CONVECTION MODEL IN COBRA III-C

The equations of the mathematical model for fluid transport are derived by using the assumptions given in the general description of the codes, and by applying the conservation equations to a segment of arbitrary subchannel (i) which is connected to another subchannel (j) as shown in Appendix C. For more than one subchannel the coupling terms are summed over all adjacent subchannels.

If the summation over all subchannels adjacent to -i- is indicated by $\sum_j$ we obtain the mass balance equation as; (App. C)

$$A_i \frac{\partial C_i}{\partial t} + \frac{\partial m_i}{\partial x} = - \sum_{j=1}^{N} W_{ij} \qquad (3.1)$$

Where ρ_i, Ai, mi, W_{ij} are density, cross-sectional area, mass flow rate, and diversion crossflow between adjacent subchannels respectively, the subscripts i, and j denote the sub-

channel identification numbers.

Equation (3.1) gives the net rate of change of subchannel flow in terms of diversion crossflow per unit length. The turbulent crossflow does not appear because it does not cause a net flow change as indicated in section III-A.

The Energy balance is given in equation below; (App. C).

$$\frac{1}{U_i''}\frac{\partial h_i}{\partial t} + \frac{\partial h_i}{\partial x} = \frac{q_i'}{m_i} - \sum_{j=1}^{N}(h_i - h_j)\frac{w_{ij}}{m_i} - \sum_{j=1}^{N}(t_i - t_j)\frac{c_{ij}}{m_i} + \sum_{j=1}^{N}(h_i - h^*)\frac{w_{ij}}{m_i} \qquad (3.2)$$

Where, U_i'', h_i, q_i', w_{ij}', h^* are the effective enthalpy thermal velocity, enthalpy, that thermal conduction term, turbulent crossflow between adjacent subchannels, diversion crossflow between adjacent subchannels, and enthalpy carried by diversion crossflow respectively.

The first two terms on the left side of equation (3.2) give the transient and spatial rate of change of enthalpy. These are convective terms with a transport enthalpy velocity. Since the transport velocity represents the effective velocity for energy transport, the time change of energy is related to this velocity. The right side of eq (3.2) contains three terms for thermal energy transport in a rod bundle fuel element. The first term on the right hand side gives the rate of energy change, the second term is related to the turbulent enthalpy transport between all adjacent subchannels. Here the turbulent mixing term W_{ij}' is defined through the empirical correlations (COBRA-III-C) Appendix C, and is analogous to eddy diffusion.

The third term accounts for the thermal conduction mixing and thelast term accounts for thermal energy carried by diversion crossflow between all adjacent subchannels. The last term depends on the enthalpy transport carried by diversion crossflow.

Axial Momentum Equation (App. C) is given by;

$$\frac{1}{A_i}\frac{\partial m_i}{\partial t} - 2U_i\frac{\partial \rho_i}{\partial t} + \frac{\partial p_i}{\partial x} = -\left[\frac{m_i}{A_i}\right]^2\left[\frac{V_i' f_i \phi_i}{2D_i} + \frac{K_i V_i'}{2\Delta x} + \frac{\partial V_i'}{\partial x}\right]$$

$$- g\rho_i\cos\theta - f_T\sum_{j=1}^{N}(U_i - U_j)\frac{W_{ij}'}{A_i} + \sum_{j=1}^{N}(2U_i - U^*)\frac{W_{ij}'}{A_i} \qquad (3.3)$$

here; U_i, p_i, V_i', f_i, ϕ_i, K_i, D_i, g, f_T, U^* are effective momentum velocity, pressure, effective specific volume for momentum, friction factor, friction multiplies, spacer losses coefficient, diameter, gravitational constant, turbulent mixing factor and effective velocity carried by diversion crossflow.

Equation (3.3) contains terms governing the axial pressure gradient in a subchannel. These are frictional, spatial, accelarational and elevational components of the pressure gradient, given in the right siole of eq. (3.3) respectively. The fourth term accounts for the momentum due to the turbulent crossflow and tends to equalize the velocities of adjacent subchannels, containing the turbulent mixing factor to equalize the turbulent transport of enthalpy and momentum. The last term including the diversion crossflow accounts for the momentum changes in subchannels due to changes in velocities carried by the diversion crossflow between all interconnected subchannels.

Computation of cross flow between the subchannels of an assembly requires a different formulation of the transverse momentum balance equation. Hence at any aqial level there will be pressure gradients leading to transvers flow in the presence of blockages around the bundle circumference.

Thus the subchannel thermal-hydraulic code COBRA III-C considers a transverse momentum balance equation for the small gaps between the rods (Fig. C-4, App.C). The transverse momentum equation is given by (eq. C.36, App. C).

$$\frac{\partial W_{ij}}{\partial t} + \frac{\partial (W_{ij}\ U^*)}{\partial x} + \left(\frac{s}{l}\right) c_{ij} W_{ij} = (p_i + p_i) \left(\frac{s}{l}\right) \qquad (3.4)$$

Equation (3.4) accounts for the transverse momentum balance. The first term on the left side represents the temporal change of the transverse momentum and the second term the spatial accelaration of the crossflow. The last term on the left side gives the frictional force, and the term on the right siole represents the pressure differences due to the crossflow.

III-B-ii. CONVECTION MODEL IN TERHID

Convection Model of TERHİD considers the conservation equations of mass, energy and momentum for a given control volume with the relevant conserved quantities (App. D). The equations are derived for single channel with the required assumptions given in Appendix D.

The continuity equation is given by (App. D)

$$A_i \frac{\partial \rho_i}{\partial t} + \frac{\partial m_i}{\partial z} = 0 \qquad (3.5)$$

Where A_i, $_i$, m_i, are cross sectional area, density of the fluid, and mass flow rate respectively.

Equation (3.5) gives the net rate of change of flow in the flow channel in terms of density and flow rate.

The energy balance is given as; (App. D)

$$\frac{1}{V_i} + \frac{\partial h_i}{\partial t} + \frac{\partial h_i}{\partial z} = \frac{q_i'}{m_i} \tag{3.6}$$

Where, V_i, h_i, q_i' are fluid velocity within the channel, enthalpy of the fluid, and heat addition per unit length from the fuel plate to the coolant.

The terms on the left side of eq. (3.6) represent the temporal and spatial rate of change of enthalpy. The time change of energy is related to the velocity of the fluid. The only term on the right side is the power-to-flow ratio in a channel and gives the rate of enthalpy change due to the energy added to the channel.

The momentum balance (eq. D.16. App. D) is given by

$$\frac{\partial p_i}{\partial z} = g\ \rho_i + 2\ V_i\ \frac{\partial \rho_i}{\partial t} + \left[\frac{m_i}{A_i}\right]^2 \frac{\partial (1/\partial \rho_i)}{\partial z} - \frac{F_i}{A_i} - \frac{1}{A_i}\ \frac{\partial m_i}{\partial t} \tag{3.7}$$

Where p_i, g, V_i, F_i, denotes pressure, gravitational constant, fluid velocity, and frictional force losses within the channel. The pressure gradient terms are given on the right side of eq. (3.7); these are, the force acting to the flow area due to the mass weight of the fluid, the accelara-

tional and frictional pressure gradients. The second and the last term on the right side account for the transient components of the pressure gradient.

III-B-iii. SUMMARY AND COMPARISON OF CONVECTION MODELS OF THE CODES

COBRA-III-C as compared with TERHİD draws a complex picture in convection model. This complexity is due to the subchannel analysis and the variation in hydraulic conditions among the various subchannels in the presence of crossflows.

The equations used in for the fluid transport in TERHID are similar to COBRA-III-C except the crossflow terms, and the turbulent mixing factor in energy balance equation, of frictional losses in momentum equation, and the additional conservation equation of transverse momentum balance.

TERHID solves the coolant enthalpy and pressure differences by using the equations (3.5) through (3.7) and the temperature of the coolant might be found with the use of the calculated enthalpy from eq. (3.6).

COBRA III-C solves the pressure difference, enthalpy, fluid temperature, by using the equations (3.1) through (3.4).

Both codes, COBRA-III-C and TERHID, use finite difference procedure for solving the equations for the fluid transport. The main difference between COBRA III-C and TERHID exists by assuming the flow direction.

TERHID assumes a downward flow which provides the disadvantages with the need for sealing the reactor plug, or

cover, against the maximum pump discharge pressure. On the other hand COBRA-III-C assumes any direction. However the upward flow provides the advantage of natural circulation.

CHAPTER IV

NUMERICAL APPLICATION

In this section the numerical solutions obtained using COBRA III-C and TERHİD will be presented.

The first part includes the application of the problem solved in TERHİD to the program COBRA III-C.

In the second part, using various time steps the effect of the time increments on the temperature solutions is analysed.

A comparison of the numerical solutions for identical problems using both programmes take place in the third part. The comparison is carried out for the same time steps in both programmes, including the forcing functions of heat flux power, temperature, and mass flow at a given time.

IV-A. APPLICATION OF A TRANSIENT PROBLEM TO TERHID AND TO COBRA III-C

As explained in the preceeding sections the computer program COBRA III-C makes the thermal-hydraulic analysis of rod bundle nuclear fuel element subchannels during steady state and transient conditions and computes the flow and enthalpy in the subchannels and temperature distribution within the fuel, fuel regions, cladding and within the channels.

The computer program TERHID makes the steady and transient state thermal-hydraulic calculations of single channel reactors, and calculates the temperature distributions within the fuel, cladding and coolant and the pressure differences from the inlet up to the outlet.

Since COBRA III-C makes subchannel analysis its convective model considers the effect of the crossflows between adjacent subchannels. Hense it includes mixing which results from the convective transport between interconnected subchannels resulting from both turbulent and diversion crossflow. Accordingly to the subchannel analysis a single channel may interact with up to four adjacent subchannels.

Due to the formulation of the subchannel analysis, considerations and the dependency of the required subchannel informations of the program COBRA III-C, the problem applied to single channel program TERHID can not be calculated without making some modifications on the model of the problem.

The single channel problem solved in TERHID can only be solved with the computer program COBRA III-C as a two equivalent subchannel problem.

On the other hand, to hold the single channel sense of the problem, the interactions between the two subchannels (between the interconnected channels) must be equalized to zero, as if there is no net flow crossing the subchannel boundary.

For this purpose a minimum value is supplied for the required mixing correlation factor. Then the transient step solutions of COBRA III-C can be compared using the single channel problem of TERHID. Thus the transient problem of TERHID is applied to COBRA III-C by forming subchannels and

required data in the manner as mentioned above.

The subchannel lagout is shown in Figure IV-1 and the input parameters are given in Table IV-1-a and in Table IV-1-b.

As obtained from Tables IV-1-a and IV-1-b, the system properties of the codes are the same, but the units input and output different. Therefore they are expressed in different units.

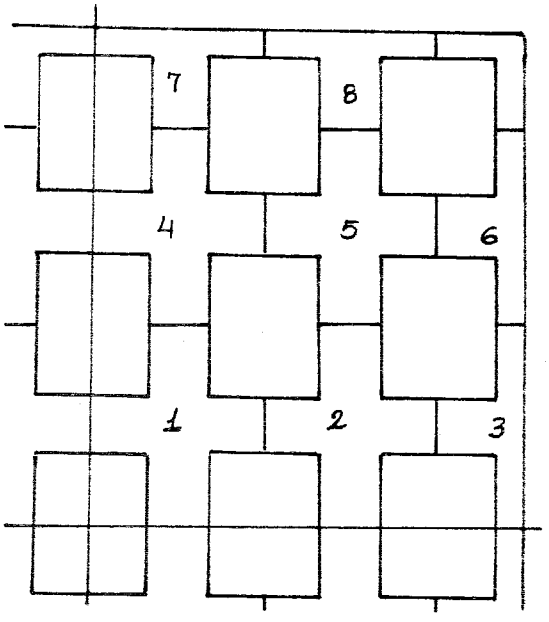

FIGURE IV-1. Subchannel layout for a 1/4 Section of symmetry

TABLE IV-1-a

Input Parameters for the problem solved by the programme COBRA III-C

Fuel conductivity	96.48 Btu/hr.ft ^{o}F
Fuel specific heat	0.1767 Btu/lb ^{o}F
Fuel density	1186.2 lb/ft^{3}
Fuel thickness	0.02 in
Cladding conductivity	121.32 Btu/hr.ft.^{o}F
Cladding specific heat	0.2140 Btu/lb.^{o}F
Cladding density	169.0 lb/ft^{3}
Cladding thickness	0.0150 in
Friction factor	f = 0.047 Re$^{-0.2}$
Heat flux distribution	X/L Relative flux
	0.0 0.165
	0.1 0.432
	0.3 0.846
	0.4 0.960
	0.5 1.000
	0.6 0.960
	0.7 0.846
	0.8 0.665
	0.9 0.432
	1.0 0.165
Momentum turbulent factor	0.5
Transverse momentum Parameter (S/L)	0.5
Turbulent mixing paraneter	β = 0.01
Channel orientation	0^{o}
Momentum turbulent factor	0
Channel length	23.47 in.
no.of axial nodes	60
no.of time steps	from 5 to 260
Total transient time	5.202 sec.
Allowable iterations	30
Avg.heat flux	0.034002 Million Btu/hr.ft^{2}

TABLE IV-1-a(continued)

Input Parameters for the problem solved by the program COBRA III-C

Mass velocity	0.308 Mlb/hrft^2
System pressure	2000.0 PSI
Inlet temperature	98.6 ^oF
Forcing function for heat flux	Time (sec) / Heat flux factor 0.000 / 1.000 0.040 / 1.000 0.041 / 0.800 30.000 / 0.800
For convection heat transfer coefficient Dittlus-Boelter correlation is used.	

TABLE IV-1-b

Input Parameters for the problem solved by the programme TERHİD

Fuel conductivity	167.0 W/m°C
Fuel density	19000.0 kg/m^3
Fuel specific heat	740.0 J/kg°C
Fuel witdhness	69.698 mm
Fuel thickness	0.508 mm
Fuel length	596.138 mm
Cladding conductivity	210.0 W/m°C
Cladding density	2707.0 kg/m^3
Cladding specific heat	896.0 J/kg°C
Cladding thickness	0.381 mm
Channel witdhness	69.9 mm
Channel thickness	6.476 mm
The extrapolated length of neutron flux	35.2 mm
Mass flow rate	417.275 kg/sn.m^2
Inlet Temperature	37°C
Power	8926.0 W
Friction factor	ff = 0.047 Rc$^{-0,2}$
Heat flux distribution	Z/H Q(n.)/Q(0.)
	0.0 0.165
	0.1 0.432
	0.3 0.846
	0.4 0.960
	0.5 1.000
	0.6 0.960
	0.7 0.846
	0.8 0.665
	0.9 0.432
	1.0 0.165

IV-A- THE TEMPERATURE CHANGE WITH TIME AT SOME TIME STEPS.

The time step determination in TERHİD depends on the channel length, fluid velocity, and on the number of axial nodes. Therefore the calculations of TERHİD is carried out for a defined time step. But the computer programme COBRA III-C is able to consider the transient problem using different time steps Δt. The required data for the different step calculations are the total calculating transient time, and the number of time steps.

To carry out the calculations during the identical transient time using both computer programmes the value obtained for the total calculating transient time is 5.202 sec.

In COBRA III-C, during the same transient time t=5.202 sec. the number of time steps are changed. The variations of results using different time increments are intercompared, with the change of inlet heat flux between 0.040 sec. and 0.041 sec. by a factor of 0.800.

The radially fuel centerline temperatures at t=1.3050 sec., t=2.601 sec., and t=4.1616 sec. with the use of different time increments are given in Tables IV-2, IV-3 and IV-4. respectively.

As given in Table IV-2 at t=1.3050 sec. the values of fuel centerline temperatures from time step 1.0 sec. up to time step 0.6 sec. are obtained by interpolation. The value of the fuel centerline temperature obtained using time increment of 0.09 sec. and 0.02 sec. are almost the same. However the value of fuel centerline temperature obtained for time increment of 0.6 sec. is 0.8 ^{o}F more than the value obtained for time increment 0.02 sec.

TABLE IV-2

The fuel centerline temperatures at t=1.3050 sec. with different time steps in COBRA III-C

t=1.3050 sec.	
Time Steps t sec,	Temperature ^{o}F
1.0	167.3*
0.9	166.9*
0.8	166.5*
0.7	166.2*
0.6	166.1
0.5	166.0
0.4	165.6
0.3	165.5
0.2	165.4
0.1	165.4
0.09	165.3
0.08	165.3
0.07	165.3
0.06	165.3
0.04	165.3
0.03	165.3
0.02	165.3

* Values obtained by interpolation

TABLE IV-3

The fuel centerline temperatures at t=2.601 sec. using different time steps in COBRA III-C

t=2.601 sec.	
Time Steps Δt [sec.]	Temperature [°F.]
1.0	163.1
0.9	162.9
0.8	162.7
0.7	162.5
0.6	162.4
0.5	162.3
0.4	162.1
0.3	161.9
0.2	161.8
0.1	161.7
0.09	161.6
0.08	161.6
0.06	161.6
0.04	161.6
0.03	161.6
0.02	161.6

TABLE IV-4

The fuel centerline temperatures at t=4.1616 sec. using different time steps in COBRA III-C

t=4.1616 sec.	
Time Steps Δt |sec.|	Temperature |°F.|
1.0	160.5
0.9	160.5
0.8	160.3
0.7	160.2
0.6	160.1
0.5	160.0
0.4	159.9
0.3	159.7
0.2	159.6
0.1	159.6
0.09	159.6
0.08	159.6
0.07	159.6
0.06	159.6
0.04	159.6
0.03	159.6
0.02	159.6

TABLE IV-5

The time required for the completion of 50 % and 90 % of the total fuel centerline temperature change for different time steps

Time steps Δt |sec.|	The time required for 50 % of the total change |sec.|	The time required for 90 % of the total change |sec.|	Total fuel-centerline temperature change °F at t=5.202 sec. for some time steps.
1.0	1.6	4.0	13.60
0.9	1.4	3.7	
0.8	1.3	3.7	
0.7	1.3	3.7	13.80
0.6	1.3	3.7	
0.5	1.3	3.6	
0.4	1.2	3.5	
0.3	1.2	3.4	
0.2	1.2	3.4	14.00
0.1	1.1	3.4	14.10
0.09	1.1	3.4	
0.08	1.1	3.4	
0.07	1.1	3.4	
0.06	1.1	3.4	
0.04	1.1	3.4	
0.03	1.1	3.4	
0.02	1.1	3.4	

As given in Table IV-3 at time t=2.601 sec. the values of the fuel centerline temperatures obtained using time increments of 0.09 sec. and 0.02 sec. are almost the same. The required time for fluid to go through one node is 0.04 sec. The value obtained using that time step is 0.1°F and 0.2°F less than the value obtained using time increments of 0.1 sec. and 0.2 sec. respectively. However using time increment 1.0 sec. the value of the fuel centerline temperature is increased by the value of 1.5°F compared with time step 0.04 sec.

At time t=4.1616 sec. (Table IV-4) the differences in the fuel centerline temperature for each time increments changes between 0.2°F and 0.1°F. The fuel centerline temperature obtained using time increments of 0.09 sec. and 0.02 sec. are again almost the same. However the value obtained in the fuel centerline temperature using time step 0.02 sec. is 0.9°F, 0.7°F, 0.6°F, 0.4°F less than the values obtained for time increments of 0.1 sec., 0.8 sec., 0.7 sec., and 0.4 sec. respectively.

The time required time for the completion of the 50 % and 90 % of the total fuel centerline temperature changes for different time increments and the total temperature changes at some time steps are given in Table IV-5.

The values obtained in the total fuel centerline temperature change for time increments of 1.0 sec. and 0.9 sec. is 13.60°F, for time increments of 0.7 sec. and 0.3 sec. this value increases to 13.80°F. Using time increments of 0.1 sec. and 0.02 sec. the total fuel centerline temperature change rises to 14.10°F. Thus different steady state values are reached. The required time for the completion of 50 % of the entire total change using time increments of 0.1 sec. and 0.02 sec. is 1.1 sec. and for the completion of 90 % of the total change the time requisite is 3.4 sec.

The solutions indicate that in some cases the temperature changes are so close, that any important differences are obtained. Such as using time increments 0.1 sec. and 0.02 sec. almost identical result's are obtained. For time step 0.2 sec. compared with the time increment 0.04 sec., which corresponds the required time for the fluid to cover the node length, the obtained difference is not important compared the differences of time increments 1.0 sec. However in some cases the temperature difference get less sensitive; like $1.5^{o}F$ as obtained using time increments of 1.0 sec and 0.02 sec. Therefore only fuel centerline temperature changes with time for time increments of 1.0 sec. and 0.02 sec. are compared in Figure IV-2., and the fuel centerline temperature changes as a function of time steps are shown in Figure IV-3.

As shown in Figure IV-2 and obtained from the solutions, the result obtained for time step 1.0 sec. is not sufficiently sensitive and the exact steady state value is not reached during 5.202 sec. However using time increments of 0.1 sec. up to 0.02 sec., the obtained solutions are more sensitive than using time increment of 1.0 sec. down to 0.3 sec. and the entire total change is completed in 5.202 sec.

These differences obtained in the fuel centerline temperature change using different time increments is due to the performation of the transient calculation. The transient calculations are performed over the channel length for a time step. Δt. The transient finite difference terms are evaluated from the solutions for the previous time step and this procedure continous, following the whole transient. Therefore for increased values of the time increments the transient solutions are not sensitive enough.

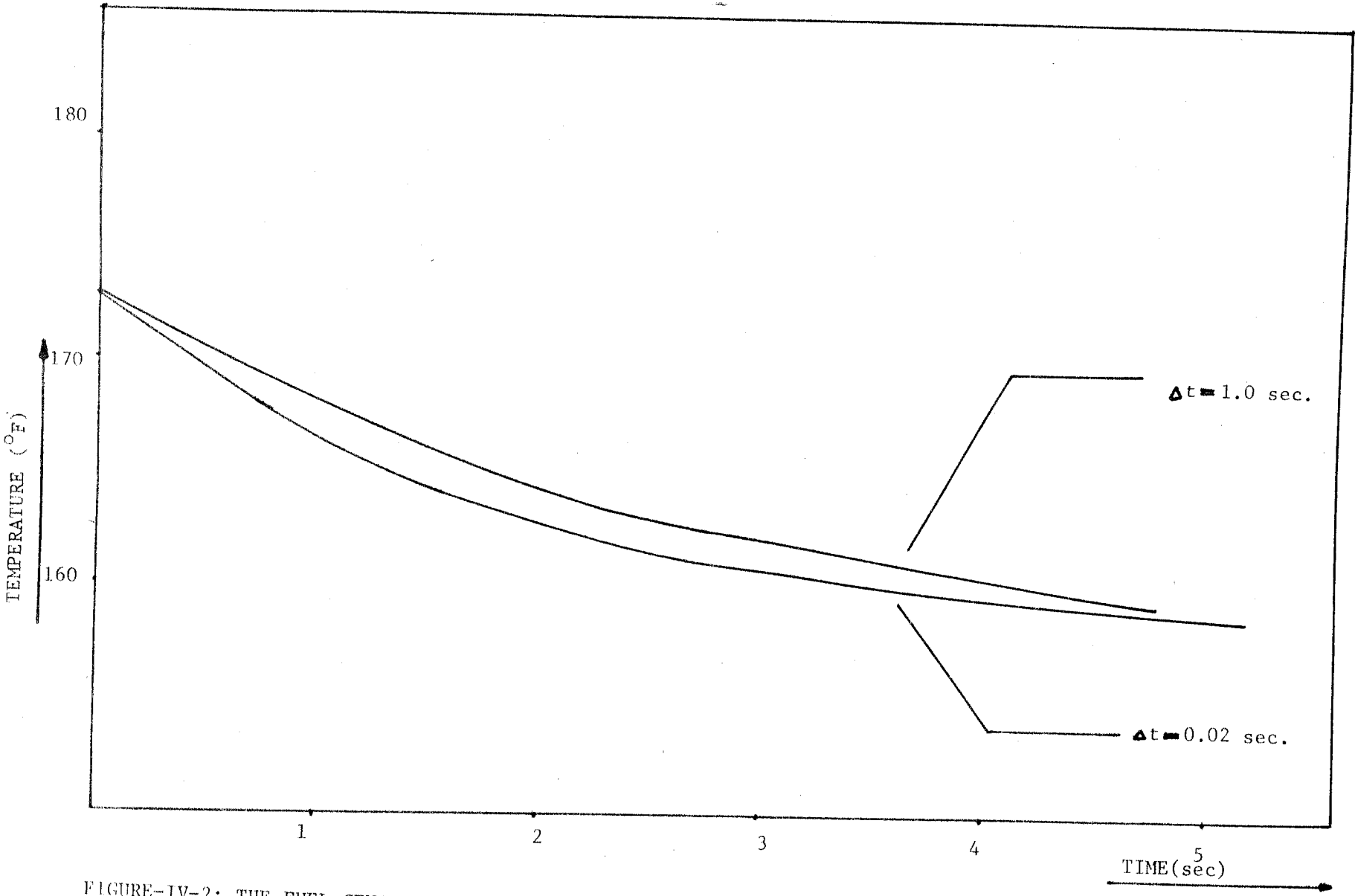

FIGURE-IV-2: THE FUEL CENTERLINE TEMPERATURE CHANGE WITH TIME

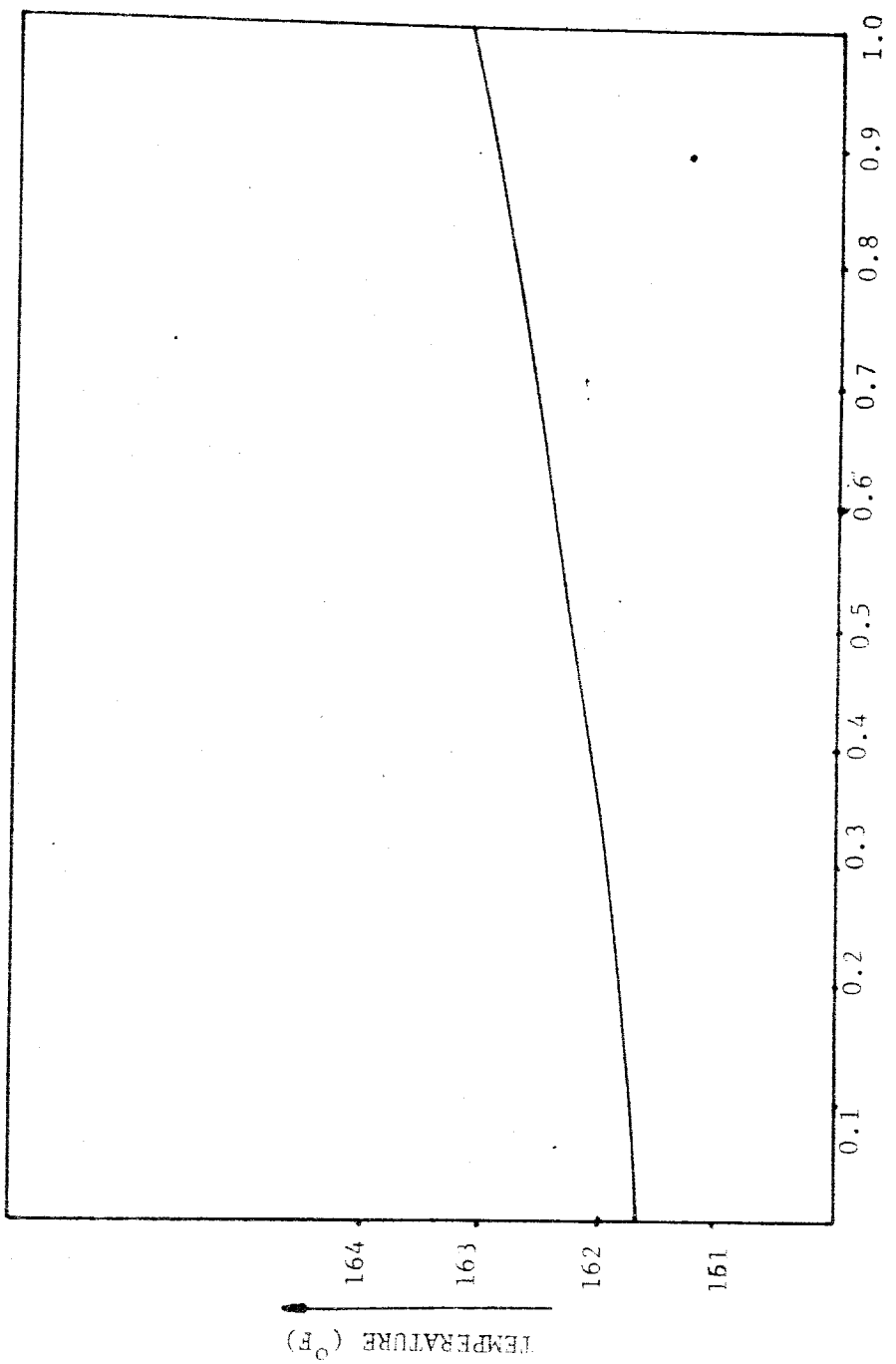

FIGURE-IV-3: THE FUEL CENTERLINE TEMPERATURE CHANGES USING DIFFERENT TIME INCREMENTS.

IV-C- COMPARISON OF THE TRANSIENT PROBLEM OF COBRA III-C AND OF TERHİD AND RESULTS

a- COBRA-III-C-Heat flux changes with time at t=0.041 sec. by the heat flux factor of 0.800
TERHİD-Power changes with time at t=0.041 sec. by the power factor of 0.800
The time interval used by TERHİD for the Previous problem is 0.236 sec.

The corresponding time step of the computer program COBRA III-C to the computer program TERHİD, during the same transient time 5.202 sec. is 0.236 sec. The calculated fuel center temperature distributions at t=0.236 sec. with both thermal-hydroulic programmes are given in Table IV-6. and the fuel center temperature distribution is given in Figure IV-4.

According to the solutions of TERHİD the fuel center temperature is reduced from 76.6°C to 69.5°C. The total fuel center temperature change is 7.10°C. The 50 % and 90 % of the total change are completed at 1.0 sec and 3.3 sec respectively.

On the other hand as obtained from Table IV-6 the total change of COBRA III-C is 7.8°C. To complete the 50 % and 90 % of the total change 1.2 sec. and 3.4 sec. are taken.

Taking care the differences in the total changes between both programmes, the time difference for the percent of the total changes are 0.2 sec. and 0.1 sec.

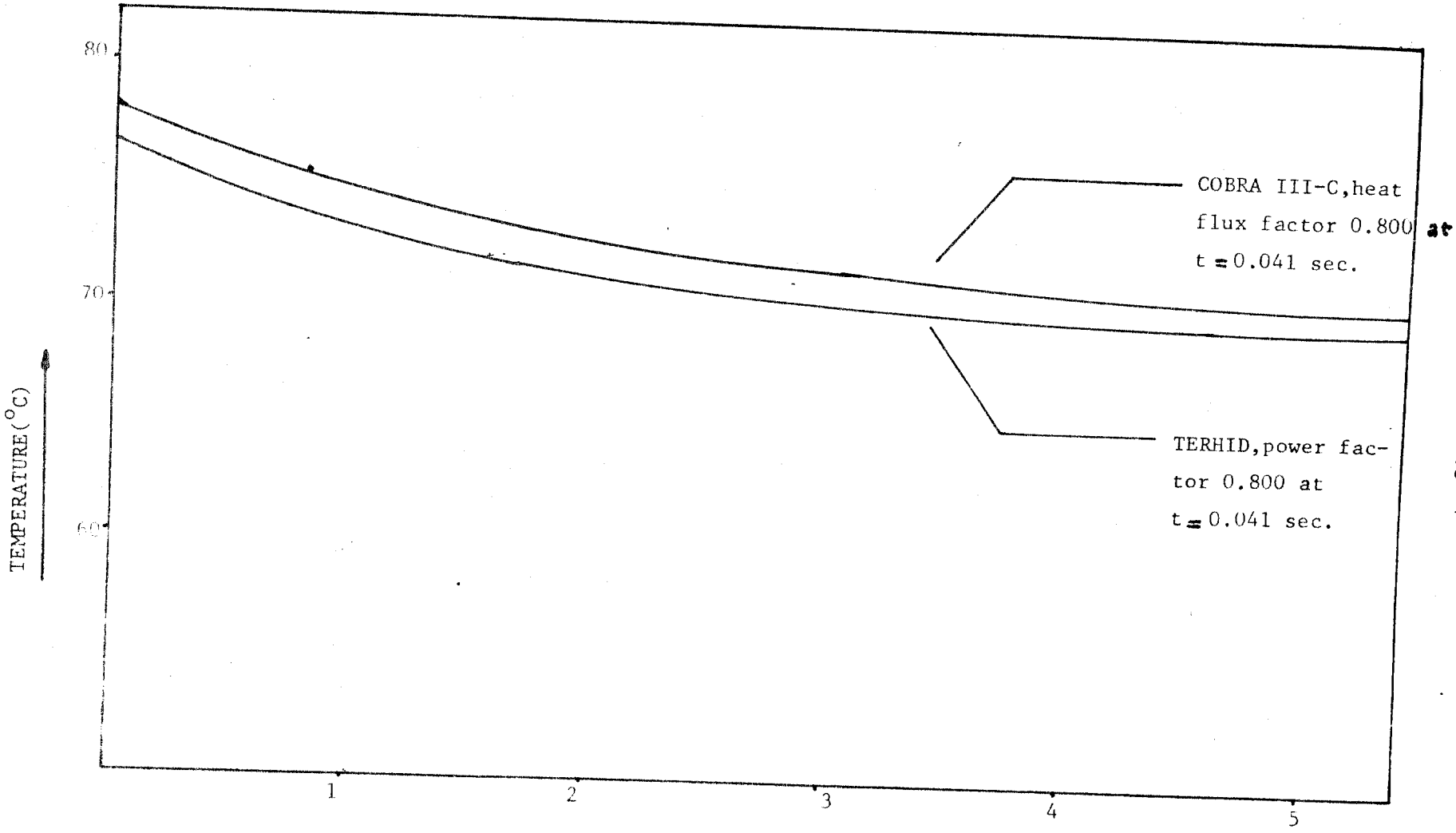

FIGURE-IV-4: THE FUEL CENTERLINE TEMPERATURE CHANGE WITH TIME DUE TO THE POWER CHANGE IN TERHID AND DUE TO THE HEAT FLUX CHANGE IN COBRA-III-C.

TABLE IV-6

Change of fuel centerline temperature with time

COBRA-III-C	Heat flux changes at t=0.041 sec. by a factor of 0.800 and Δt=0.236 sec.
Time [sec.]	Fuel Center Temperature [°C]
0.0	78.4
0.473	76.5
0.946	75.1
1.419	73.9
1.892	73.6
2.365	72.4
2.838	71.9
3.311	71.5
3.784	71.2
4.257	70.9
4.730	70.7
5.202	70.6
TERHİD	Power changes at t=0.041 sec. by a factor of 0.800 and Δt=0.236 sec.
Time [sec.]	Fuel Center Temperature [°C]
0.0	76.6
0.473	74.6
0.946	73.2
1.419	72.2
1.892	71.4
2.365	70.9
2.838	70.5
3.311	70.2
3.784	69.9
4.257	69.7
4.730	69.6
5.202	69.5

b- COBRA III-C-Inlet temperature changes with time at t=0.041 sec. by the inlet temperature factor of 0.811.
TERHİD-Inlet temperature changes with time at t=0.041 sec. by the inlet temperature factor 0.811.

The value of the reference inlet temperature of COBRA III-C, which corresponds to the value of the reference inlet temperature of TERHİD, is reduced between 0.040 sec. and 0.041 sec. from 37°C to 30°C. Accompanying the decrease in the inlet temperature, the fuel centerline temperature changes from 78.4°C to 74.4°C at the end of 5.202 sec. The change of the fuel centerline temperature for time step 0.236 sec. in both programmes are given in Table IV-7 and the temperature distribution are given in Figure IV-5.

The total temperature change in COBRA III-C is 4.0°C. The 50% and 90% of the total change are completed in 1.9 sec. and 4.0 sec. respectively.

On the other hand using computer code TERHİD the fuel center temperature is reduced from 76.6°C to 72.0°C. at the end of 5.202 sec. The total change is 4.6°C. The difference obtained in both programmes is due to the computation procedure and the required input of the heat flux in the COBRA III-C code. To complete the 50 % and 90 % of the total change the time durating of TERHİD is 1.7 sec. and 3.6 sec. respectively.

TABLE IV-7

Change of fuel centerline temperature with time

COBRA-III-C	Inlet Temperature changes at t=0.041 sec by a factor of 0.811 and Δt=0.236 sec.
Time [sec.]	Fuel Center Temperature [°C]
0.0	78.4
0.473	78.2
0.946	77.7
1.419	77.1
1.892	76.4
2.365	75.9
2.838	75.5
3.311	75.2
3.784	74.9
4.257	74.7
4.730	74.6
5.202	74.4
TERHİD	Inlet Temperature changes at t=0.041 sec. by a factor of 0.811 and Δt=0.236 sec.
Time [sec.]	Fuel Center Temperature [°C]
0.0	76.6
0.473	76.5
0.946	75.9
1.419	74.9
1.892	74.1
2.365	73.5
2.838	73.0
3.311	72.7
3.784	72.4
4.257	72.2
4.730	72.1
5.202	72.0

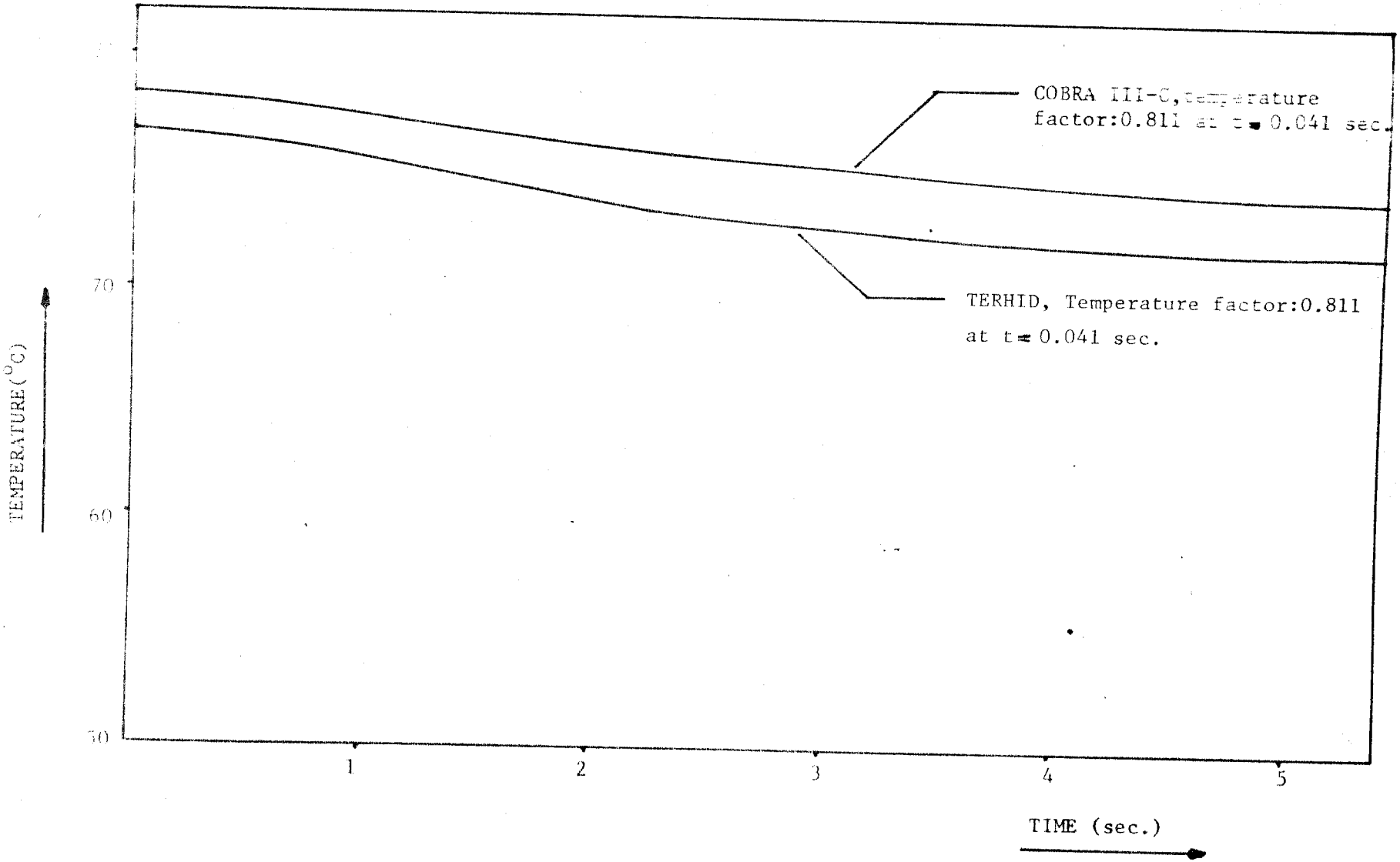

FIGURE IV-5: THE FUEL CENTERLINE TEMPERATURE CHANGE WITH TIME DUE TO THE INLET TEMPERATURE CHANGE IN COBRA III-C AND IN TERHID.

According to the calculations the difference in the total changes between both programmes is 0.6°C and the differences in the percent changes are 0.2 sec. and 0.4 sec.

c- COBRA III-C- Inlet flow changes with time at t=0.041 sec. by the inlet flow factor of 0.800
TERHİD- Inlet flow changes with time at t=0.041 sec. by the inlet flow factor of 0.800.

It is assumed that the inlet flow changes between 0.040 sec. and 0.041 sec. by the inlet flow factor 0.800 in COBRA III-C and in TERHİD. The changes in the fuel center temperature at time step Δt=0.236 sec. for both programmes are given in Table IV-8 and the fuel center temperature distributions are given in Figure IV-6.

In COBRA-III-C-the inlet flow is reduced from 0.308 M.lb/hr.ft^2 to 0.2461 M.lb/hr.ft^2 at time 0.041 sec. The fuel center temperature increases from 78.4°C to 85.7°C at the end of 5.202 sec. The total change in the fuel center temperature is 7.3°C. For the completion of the 50 % and 90 % of the total change 1.4 sec. and 3.7 sec. are taken.

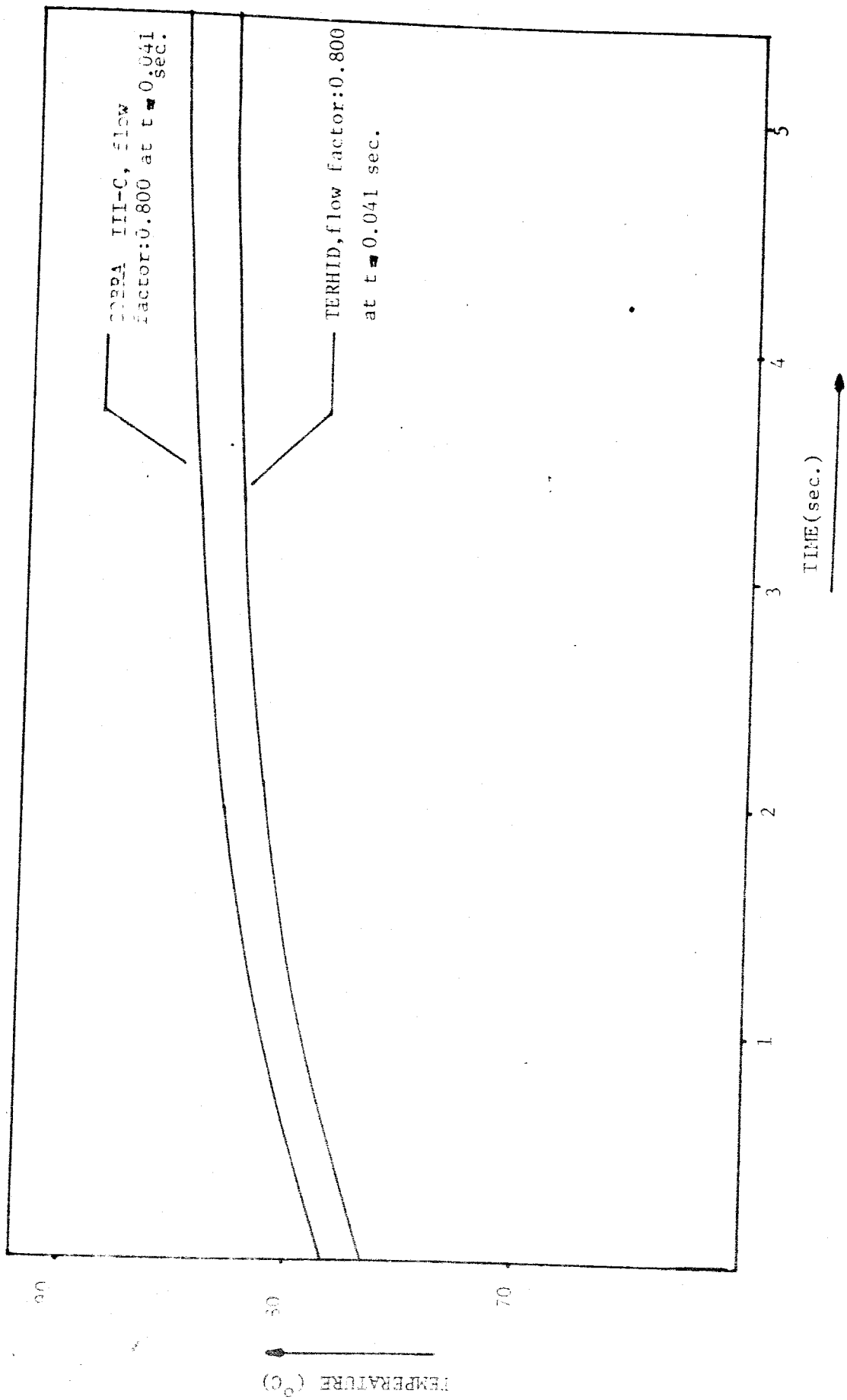

FIGURE-IV-6: THE FUEL CENTERLINE TEMPERATURE CHANGE WITH TIME DUE TO THE FLOW CHANGE IN TERHID IN CORBA III-C.

TABLE-IV-8

Change of fuel centerline temperature with time:

COBRA III-C	Inlet Flow changes at t=0.041 sec. by a factor of 0.800 and Δt=0.236 sec
Time [sec.].	Fuel Center Temperature [°C]
0.0	78.4
0.473	79.9
0.946	81.2
1.419	82.2
1.892	83.0
2.365	83.7
2.838	84.2
3.311	84.6
3.784	85.0
4.257	85.2
4.730	85.5
5.202	85.7
TERHİD	Inlet flow changes at t=0.041 sec. by a factor of 0.800, and Δt=0.236 sec.
0.0	76.6
0.473	78.2
0.946	79.4
1.419	80.4
1.892	81.2
2.365	81.8
2.838	82.3
3.311	82.6
3.784	82.9
4.257	83.1
4.730	83.3
5.202	83.4

On the other hand the reference inlet flow in TERHİD is reduced from 417.275 kg./sn.m^2 to 333.820 kg/sn.m^2 between 0.040 sec. and 0.041 sec. The fuel center temperature increases as inlet flow decreases from 76.6°C to 83.4°C at the end of 5.202 sec. Hence the total change is 6.8°C. The time durating for the completion of the 50 % and 90 % of the total change TERHİD needs 1.2 sec. and 3.5 sec. respectively.

The difference between the temperatures in COBRA-III-C are 0.1°C more than the difference between the temperatures obtained in TERHİD. Also the difference in the total change between both thermal-hydraulic programmes is 0.5°C. TERHİD completes the 50 % and 90 % of the total change 0.2 sec. earlier than COBRA III-C.

The comparison of the coolant exit temperature is carried out by changing the inlet temperature of the inflowing fluid in both programmes. It is assumed that the inlet reference temperature of the coolant in both codes is reduced from $37^{o}C$ to $30^{o}C$ between 0.040 sec. and 0.041 sec. by a factor of 0.811.

The total coolant exit temperature change obtained in TERHID is $6.80^{o}C$. The required time for the completion of 50 % and 90 % of the entire total change is 1.5 sec. and 2.5 sec. respectively.

The value obtained in the total coolant exit temperature change in COBRA III-C is $7.60^{o}C$. For the completion of 50 % and 90 % of the total change COBRA III-C requires 1.8 sec. and 2.8 sec. respectively.

At the end of 5.202 sec. the obtained exit coolant temperature difference of COBRA III-C is 6.8 % less than TERHİD. However both programmes approach asymtotically to the steady solutions from 4.2 sec.

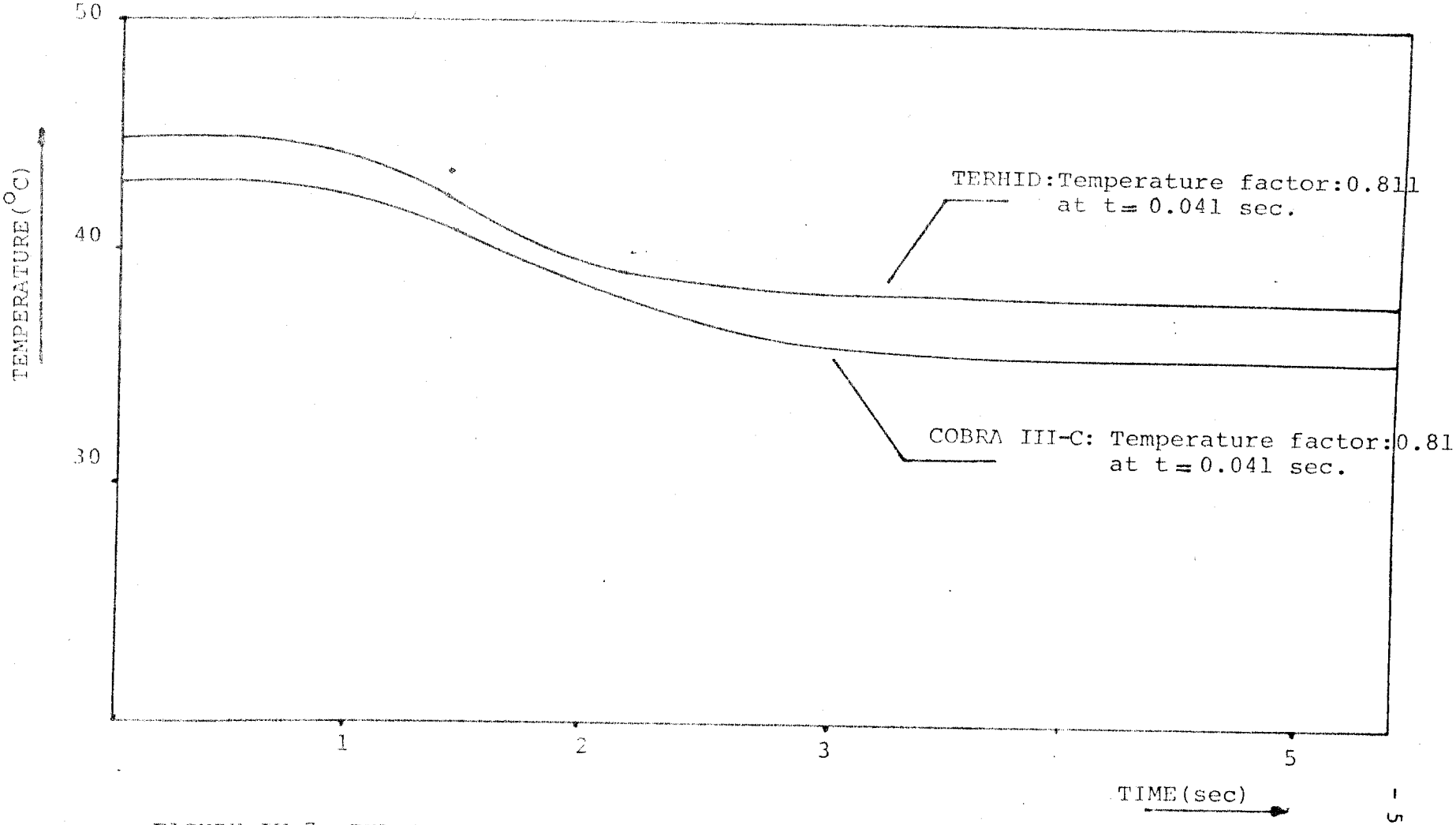

FIGURE-IV-7: THE COOLANT EXIT TEMPERATURE CHANGE WITH TIME

CHAPTER V

DISCUSSION OF THE RESULTS AND CONCLUSION

The conduction and convection models of the computer programmes COBRA III-C and TERHİD, and assumptions used in both programmes and the solutions of the two codes have been analysed.

The transient solutions of COBRA III-C for some time increments have been presented, and the solution of TERHİD for the corresponding time step to COBRA III-C has been compared. The effect of the assumptions on the numerical values in the numerical analysis has been discussed.

Several set of calculations have been carried out by using COBRA III-C and the solutions for different time increments have been compared to show the effect of time increments on the results. The results show that the fuel heat transfer model and the flow are coupled by their time responses. If the time interval between calculations is more than twice the time taken the flowing fluid in going through one node then the temperature of the fuel is changed less during the transient as compared with the identical transient time calculated with longer time increment.

As obtained from the solutions exact and more sensitive results are reached using increased time steps than the results obtained for lower number of time steps for a given total transient time. However, after some time increments the effect of the time steps on the solutions become negligible.

Another comparison of the two codes has been carried out including the transient effects of the inlet power, temperature and mass flow rate changes. The obtained results for all cases from both codes indicate that the fuel centerline temperature takes the asymptotic form and so approaches to steady state conditions. But there exists a temperature difference between both programmes. This difference might be due to the heat flux information as input and the assumption of the steady state conditions to calculate the power from the given heat flux results in approximate solutions. Therefore TERHİD provides more accurate and sensitive solutions especially for the transient calculations than COBRA III-C.

Including the computational efficiency to this, COBRA-III-C requires 32K of memory, on the other hand TERHİD requires 9K of memory. The memory requirements for both codes in addition to the solution technique depends on the number of axial and radial nodes, number of time steps of the problem. Using the same time step $\Delta t=0.236$ sec. during the same total transient time 5.202 sec. and same axial node number it is obtained that COBRA III-C spends 29 min. and TERHİD spends 35 sec. computation time.

Considering the use of the power input specially in transient state calculations, and the short time requirements to perform the calculations, for the problems corresponding to it's nature TERHİD can be prefered to COBRA III-C.

To extend the use of the program TERHİD the following additions can be made.

The time increments can be determined independently from the channel length and axial node number. The flow rate of the inflowing fluid and the channel areas is assummed to be same for all channels. the program can be arranged to

allow the calculations for different flow rates, and for variable channel areas. A subprogramme for subcooling conditions and for correlations at that conditions can be added to the programme by making the required changes in the code.

REFERENCES

Arpacı,V.S., Conduction Heat Transfer, Addison-Wesley Reading, Mass., 1966.

Aybers,N., S.Kakaç, Ş.Gençay, The Economic Comparison of Nuclear Reactors for Developing Countries. İ.T.Ü.-1974.

Borak,F., Plâka Yakıt Elemanlı Nükleer Reactor Geçici ve Sürekli Rejim Termohidrolik Analizi.

C.Gazley,JR, G.M.Harpole, et.al., Prediction of Thermal-hydraulic Performance of Gas-Cooled Fast Breeder Reactors. R-1978-EPRI-1977.

Donna,M.D., J.G. Collier, E.Hicken, H.Hoffmann, International Heeting on Reactor Heat Transfer, Karlsruhe, October, 1973.

Eckert and Irvine, Progress in Heat and Mass Transfer V.III, 1953-1969.

El-Wakil, M.M., Nuclear Heat Transport, International, Scranton, Pa., 1971.

Knudsen and Katz, Fluid Dynamics and Heat Transfer Michigan, 1953.

L.Kuipers, R.Timman, Handbuch der Mathematik Walter de Grusters. and Co. Berlin 1968.

M.K.Butler, et.al., Compilation of Program Abstracts, Argon National Laboratory, Volume III, ANL-7411.

O.E.Dwyer, Progress in Heat and Mass Transfer Volume 7, Na. Lab., New York, 1973.

O.Deublin,Lingen, Dubbel. Taschenbuch für den Mashinenbau; Waermelehre, erster Band. Springer-Verlag. Berlin-1970.

P.Nelson, C.H.Neil, Simplyfied Subchannel Model of Thermal - Hydraulic Behavior. Nucl.Sci.Eng., 1981.

Rowe,D.S., COBRA III-C: A Digital Computer Program for Steady State and Transient Thermal-Hydraulic Analysis of Rod Bundle Fuel Elements, BNWL-1695, March, 1973.

Sesonske,A., Nuclear Power Plant Analysis, U.S.A., E.C. Report TID-26241, 1973.

Weisman,J., and Browring,R.W., Methods of Detailed Thermal and Hydraulic Analysis of Water Cooled Reactors, Nuc. Sci.Eng., 57, 255-276, 1975.

William T.Sha, Robert,C.Schmitt, et.al., Boundary-Value Thermal-Hydraulic Analysis of a Reactor Fuel Rod Bundle. Nuc.Sci.Eng. 59, 140-160, 1976.

APPENDIX A

DERIVATION OF EQUATIONS FOR FUEL HEAT TRANSFER MODEL OF COBRA III - C

DERIVATION OF EQUATIONS FOR FUEL HEAT TRANSFER MODEL IN COBRA III-C

The time dependent one dimensional general conduction equation with heat generation in cyclindrical coordinate system system is given as

$$\rho c \frac{\partial T}{\partial t} = k \left[\frac{\partial^2 T}{\partial r^2} + \frac{1}{r} \frac{\partial T}{\partial r} \right] + q''' \qquad (A.1)$$

at each location -i- designated in Figure (II-1).

It should be noted that at the nodal point i=1, at the center of the rod the term $\frac{1}{r} \frac{\partial T}{\partial r}$ in equation (A.1) is indeterminate and therefore must be replaced by it's limit as $r \to 0$ (L.Kuipers-R.Timman 67). It follows from L'Hospital's rule that

$$\lim_{r \to 0} \frac{1}{r} \frac{\partial T}{\partial r} = \lim_{r \to 0} \frac{\partial T / \partial r}{\partial r} = \frac{\partial^2 T}{\partial r^2} \qquad (A.2)$$

Inserting equation (A.2) into (A.1) equation (A.1) reduce to

$$\rho c \frac{\partial T}{\partial t} = 2k \frac{\partial^2 T}{\partial r^2} + q''' \qquad (A.3)$$

To write equation (A.3) for the nodal point i=1 in finite difference form the right side and the left side of equation (A.3) is expanded into Taylor's series (K.Kuipers-R.Timman 67).

Hence:

$$T_{i+1} = T_i + \frac{\Delta r}{1!} \frac{\partial T}{\partial r} + \frac{\Delta r^2}{2!} \frac{\partial^2 T}{\partial r^2} + \ldots \qquad (A.4)$$

$$T_i = \bar{T}_i + \Delta t \frac{\Delta T}{\Delta t} \qquad (A.5)$$

where overscore (-) denotes previous time. Using the boundary condition for i=1

$$\left.\frac{\partial T}{\partial r}\right|_{i=1} = 0 \quad \text{at} \quad r=0 \tag{A.6}$$

$$\frac{\partial^2 T}{\partial r^2} = \frac{2}{\Delta r^2}\left[T_{i+1} - T_i\right] \tag{A.7}$$

Inserting equations (A.4), (A.5) into (A.3) and using the boundary condition given in (A.6) the finite difference form of equation (A.3) will be as;

$$\rho c \frac{T_1 - \bar{T}_1}{\Delta t} = 4k \frac{(T_2 - T_1)}{\Delta r^2} + q_1''' \tag{A.8}$$

Rearranging equation (A.8) the temperature at fuel center is found as; i=1

$$\rho c \frac{\bar{T}_1}{\Delta t} + q_1''' = T_1\left[\frac{4k}{\Delta r^2} + \frac{\rho c}{\Delta t}\right] - \frac{4k}{\Delta r^2} T_2 \tag{A.9}$$

To find the temperature distribution in fuel region we use equation (A.1)

For $1 < i < N$

The finite difference form of the second derivatice (Wakd) is;

$$\frac{\partial^2 T}{\partial r^2} = \frac{\left.\frac{\partial T}{\partial r}\right|_{i+1} - \left.\frac{\partial T}{\partial r}\right|_{i}}{\Delta r} = \frac{\frac{T_{i+1} - T_i}{\Delta r} - \frac{T_i - T_{i-1}}{\Delta r}}{\Delta r}$$

$$\frac{\partial^2 T}{\partial r^2} = \frac{T_{i+1} - 2T_i + T_{i-1}}{\Delta r^2} \tag{A.10}$$

$$\frac{\partial T}{\partial r} = \frac{T_{i+1} - T_{i-1}}{2\Delta r} \tag{A.11}$$

$$\frac{1}{r}\frac{\partial T}{\partial r} = \frac{1}{(i-1)\Delta r}\frac{T_{i+1} - T_{i-1}}{2\Delta r} \tag{A.12}$$

Inserting equations (A.10), (A.11), and (A.12) into equation (A.1) the temperature distribution in fuel regions for the nodal points $1 < i < N$ are found.

$$\rho c \frac{T_i - \bar{T}_i}{\Delta t} = k\left[\frac{T_{i+1} - 2T_i + T_{i-1}}{\Delta r^2} + \frac{1}{2(i-1)\Delta r^2}(T_{i+1} - T_{i-1})\right] + q'''_i \tag{A.13}$$

Rearranging equation (A.13)

$$\rho c \frac{T_i}{\Delta t} + q'''_i = \left[\frac{\rho c}{\Delta t} + \frac{2k}{\Delta r^2}\right] T_i - \left[\frac{k}{\Delta r^2} + \frac{k}{2(i-1)\Delta r^2}\right] T_{i+1} + \left[\frac{k}{2(i-1)\Delta r^2} - \frac{k}{\Delta r^2}\right] T_{i-1} \tag{A.14}$$

Temperature distribution at the fuel-clodding interface condition. For i=N

Using equation (A.1) and the boundary condition at fuel-cladding interface

The boundary condition is given by

$$-k\frac{\partial T}{\partial r} = hgap\ (T_N - T_{N+1}) \tag{A.15}$$

and using the Taylor series expansion for i=N

$$T_{N-1} = T_N + \frac{\Delta r}{1!}\frac{\partial T}{\partial r} \quad \frac{\Delta r^2}{2!}\frac{\partial T}{\partial r^2} \tag{A.16}$$

$$T_N = \bar{T}_N + \Delta t \frac{\partial T}{\partial t} \tag{A.17}$$

Rearranging equations (A.16) and (A.17) and inserting into equation (A.1) with the use of the boundary condition given in equation (A.15)

$$\rho c \frac{T_N - \bar{T}_N}{\Delta t} = k \left[2 \frac{T_{N-1} - T_N}{\Delta r^2} + \frac{2}{(N-1)\Delta r} hgap(T_N - T_{N+1}) - \frac{1}{(N-1)\Delta r} hgap(T_N - T_{N+1}) \right] + q'''_N \tag{A.18}$$

Rearranging equation (A.18)

$$\rho c \frac{T_N}{\Delta t} + q'''_N = \left[\frac{2k}{\Delta r^2} - \frac{\rho c}{\Delta t} - \frac{k.hgap}{\Delta r(N-1)} \right] T_N - \frac{2k}{\Delta r^2} T_{N-1} + \left[\frac{k.hgap}{(N-1)\Delta r} \right] T_{N+1} \tag{A.19}$$

For the cladding temperature at i = N+1.

The cladding is treated as lumped parameter node. So that the conductance through the cladding is lumped (Arpacı, V.)

The heat transfer equation for the cladding is given as;

$$\rho c \frac{\partial T}{\partial t}\Big|_{i=N+1} = q_{gap_{cond.}} - q_{coolant_{surface}} \tag{A.20}$$

$q_{gap_{cond}}$ denotes the heat conducted from the gap to the cladding and $q_{coolant_{surface}}$ denotes the heat conducted from the cladding to the coolant.

The heat conducted through the gap to the cladding is given as;

$$q_{gap_{cond}} = \frac{h_{gap}}{t_{clad}} \frac{r_N}{r_{N+1}} (T_N - T_{N+1}) \qquad (A.21)$$

Where t_{clad} is cladding thickness.

The heat transfered from the cladding to the coolant

$$q_{coolant_{surface}} = h_{surf} \frac{1}{t_{clad}} (T_{N+1} - T_f) \qquad (A.22)$$

where T_f is the coolant temperature and h_{surf} surface heat transfer coefficient.

From equations (A.20), (A2.1) and (A.22) the finite difference equation for the cladding may be wirtten as;

$$\rho c \frac{T_{N+1}}{\Delta t} + q'''_{N+1} = \left[\frac{h_{surf}}{t_{clad}} + \frac{h_{gap}}{t_{clad}} \frac{r_N}{r_{N+1}} - \frac{\rho c}{\Delta t} \right] T_{N+1} - \frac{h_{surf}}{t_{clad}} T_f - \frac{h_{gap}}{t_{clad}} \frac{r_N}{r_{N+1}} T_N \qquad (A.23)$$

At the fuel-cladding interface an effective heat transfer coefficient is used, to combine the conductance of the cladding and the gap.

$$\frac{1}{h_{gap}} = \frac{1}{h_{gap_{cond.}}} + \frac{t_{clad}}{k_{clad}} \qquad (A.24)$$

The fuel power density is defined in terms of equivalent impressed flux as if there is no fuel model. The total

power is given as.

$$\rho c \frac{\partial T}{\partial t} \pi \cdot \frac{D_f^2}{4} \cdot \Delta x = q''' \cdot \pi \cdot \frac{D_f^2}{4} \Delta x - q'' \cdot \pi \cdot D \cdot \Delta x \qquad (A.25)$$

where D_f is the fuel pellet diameter, and q" is the heat flux. The power density is found by assumming equation (A.26) in steady state conditions, hence the left side of equation (A.26) is equal zero

$$q''' = q'' \frac{4D}{D_f} \qquad (A.26)$$

D is the fuel rod diameter including the cladding.

The plate fuel is considered to be equivalent to the rod fuel such as the thickness of the plate is taken equal to the radius of the fuel rod. The thickness is in this case the distance from the outer surface of the cladding to the center-line of the plate Figure (A-1).

And the power density defined as for the rod.

$$q''' = q'' \frac{\pi \cdot D \cdot \Delta x}{\frac{D_f}{2} \cdot \pi \cdot D \cdot \Delta x} \qquad (A.27)$$

where $\pi.D$ is the width of the plate, D, is the thickness of the plate fuel including the cladding (Figure A-1).

The plate fuel is considered to be equivalent to rod fuel. The thickness of the plate is taken equivalent to the radius of the rod, and the circumference of the rod is taken equal to the width of the plate the power density for the plate fuel is

$$q''' = q'' \cdot \frac{2}{D_f} \qquad (A.28)$$

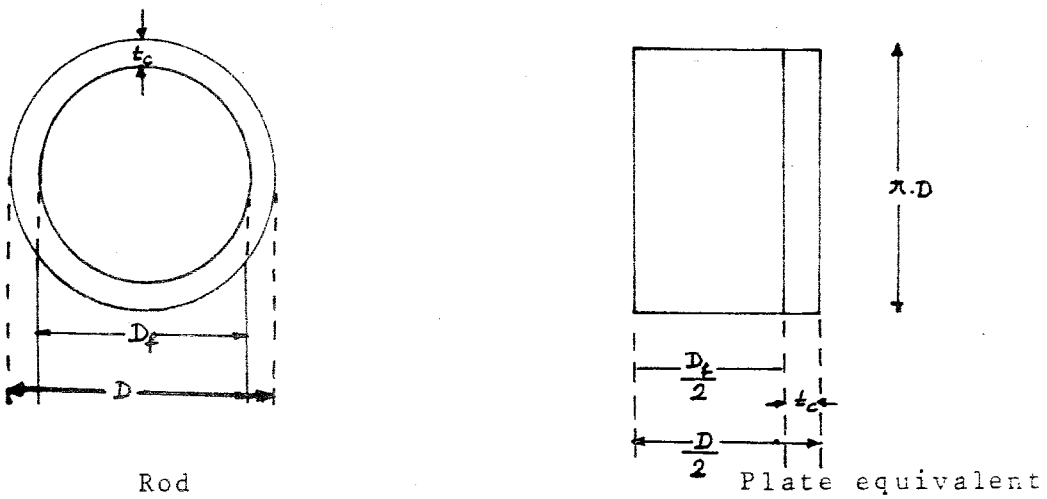

FIGURE A-1

For the plate type fuel element the same set of equations are used as for the cyclindrical fuel element (equations A.1 - A.24) except the radial coordinate term $\frac{1}{r}\frac{\partial T}{\partial r}$ used for the cyclindrical fuel type.

APPENDIX B

DERIVATION OF EQUATIONS FOR FUEL HEAT TRANSFER MODEL OF TERHID

DERIVATION OF EQUATIONS FOR FUEL HEAT TRANSFER MODEL OF TERHID

With the use of the Lumped Parameter Technique (Arpaci Wakil-71, Holmann-76) the lumped first law of thermodynamics applied to the system (Figure II-2) reduces to

$$\frac{dE}{dt} = - q''.A_1 \qquad (B.1)$$

Making use of the definition of specific heat the left side of equation (B-1) becomes;

$$\frac{dE}{dt} = \rho_1 c_1 A_1 L_1 \frac{dT_1(t)}{dt} - q''' . A_1 L_1 \qquad (B.2)$$

Inserting equation (B.2) into (B.1) we get the lumped form of the first law of thermodynamics (Borak).

$$\rho_1 c_1 L_1 ydz \frac{dT_1(t)}{dt} = q''' L_1 ydz - q''.ydz \qquad (B.3)$$

Equation (B.3) is the governing equation of the fuel plate. The left side of equation (B.3) is the time rate of change of the heat, the first term on the right side gives the heat generation in the fuel and the second term indicates the heat conduction from the fuel to the cladding.

The heat flux in equation (B.3) is given by

$$q'' = h_1(T_1(t) - T_2(t)) \qquad (B.4)$$

where $T_1(t)$ and $T_2(t)$ are the time dependent fuel and cladding temperatures. With the definition of the heat flux equation (B.3) will be as below.

$$\rho_1 c_1 L_1 ydz \frac{dT_1(t)}{dt} = q''' .ydz.L_1 - h_1 ydz \quad T_1(t)-T_2(t) \tag{B.5}$$

Rearranging equation (B.5)

$$\frac{dT_1(t)}{dt} = \frac{q'''}{\rho_1 c_1} - \frac{h_1}{\rho_1 c_1 L_1} (T_1(t) - T_2(t) \tag{B.6}$$

where;

$$\frac{h_1}{\rho_1 c_1 L_1} = \alpha_1 \tag{B.7}$$

$$\frac{dT_1(t)}{dt} + \alpha_1 T_1(t) - \alpha_1 T_2(t) = \frac{q'''}{\rho_1 c_1} \tag{B.8}$$

The heat conduction equation for the cladding is written in the same way as written for the fuel, but without the heat generation term (Borak-79)

$$\rho_2 c_2 L_2 ydz \frac{dT_2(t)}{dt} = h_1(T_1(t)-T_2(t))ydz-h_2(T_2(t)-T_f) \tag{B.9}$$

$$\frac{dT_2(t)}{dt} = \frac{h_1}{\rho_2 c_2 L_2} (T_1(t)-T_2(t)) - \frac{h_2}{\rho_2 c_2 L_2}(T_2(t)-T_f) \tag{B.10}$$

making the definitions of α_2 and α_3

$$\alpha_2 = \frac{h_1}{\rho_2 c_2 L_2} \tag{B.11}$$

$$\alpha_3 = \frac{h_1}{\rho_2 c_2 L_2} + \frac{h_2}{\rho_2 c_2 L_2} \tag{B.12}$$

$$(\alpha_3-\alpha_2) = \frac{h_2}{\rho_2 c_2 L_2} \tag{B.13}$$

Introducing equations (B.11), (B.12) and (B.13) into (B.10), one obtains

$$-\alpha_2 T_1(t) + \frac{dT_2(t)}{dt} + \alpha_3 T_2(t) = (\alpha_3 - \alpha_2)\, T_f \qquad (B.14)$$

Equations (B.8) and (B.14) are coupled differential equations and solved with the use of commutative operators (Hildebrand-63).

With the use of linear differential operators O_i equations (B.8) and (B.14) may be written as;

$$\begin{aligned} O_1 T_1(t) + O_2 T_2(t) &= H_1 \\ O_3 T_1(t) + O_4 T_2(t) &= H_2 \end{aligned} \qquad (B.15)$$

For the commutative operators

$$\Delta_1 = \begin{vmatrix} O_1 & O_2 \\ O_3 & O_4 \end{vmatrix} \qquad (B.16)$$

$$\Delta T_1(t) = \begin{vmatrix} H_1 & O_2 \\ H_2 & O_4 \end{vmatrix} \qquad (B.17)$$

$$\Delta T_2(t) = \begin{vmatrix} O_1 & H_1 \\ O_3 & H_2 \end{vmatrix} \qquad (B.18)$$

with the definition $D = \frac{d}{dt}$ equation (B.16) is written as;

$$\Delta = \begin{vmatrix} D + \alpha_1 & -\alpha_1 \\ -\alpha_2 & D + \alpha_3 \end{vmatrix} \qquad (B.19)$$

$$\Delta = (D+\alpha_3)(D+\alpha_1) - (\alpha_2)(\alpha_1)$$

$$\Delta = D^2 + (\alpha_1+\alpha_3)D + (\alpha_1\alpha_3 - \alpha_1\alpha_2) \qquad (B.20)$$

and equation (B.17)

$$\Delta T_1(t) = \begin{vmatrix} \frac{q'''}{\rho_1 c_1} & -\alpha_1 \\ (\alpha_3-\alpha_2)T_f & D+\alpha_3 \end{vmatrix} \qquad (B.21)$$

$$T_1(t) = \frac{\alpha_3 q'''}{\rho_1 c_1} + \alpha_1(\alpha_3-\alpha_2)T_f \qquad (B.22)$$

from equation (B.18)

$$\Delta T_2(t) = \begin{vmatrix} D + \alpha_1 & \frac{q'''}{\rho_1 c_1} \\ -\alpha_2 & (\alpha_3-\alpha_2)T_f \end{vmatrix} \qquad (B.23)$$

$$\Delta T_2(t) = \frac{\alpha_2 q'''}{\rho_1 c_1} + \alpha_1(\alpha_3-\alpha_2)T_f \qquad (B.24)$$

Turning to equation (B.20) with r=D

$$r^2 + (\alpha_1+\alpha_3)r + (\alpha_1\alpha_3 - \alpha_1\alpha_2) = \Delta \qquad (B.25)$$

Taking the right side of equation (B.25) equal to zero to solve the homogenous part of the differential equation

$$r^2 + (\alpha_1+\alpha_3)r + (\alpha_1\alpha_3 - \alpha_1\alpha_2) = 0$$

$$r_{1,2} = \frac{-(\alpha_1+\alpha_3) \pm \sqrt{(\alpha_1+\alpha_3)^2 - 4(\alpha_1\alpha_3 - \alpha_1\alpha_2)}}{2} \qquad (B.26)$$

From (B.26) it can be shown that $r_{12} < 0$, hence the homogenous solution for $T_1(t)$ and $T_2(t)$ will be

$$T_{1H} = c_1 e^{r_1 t} + c_2 e^{r_2 t}$$
$$T_{2H} = d_1 e^{r_1 t} + d_2 e^{r_2 t} \qquad (B.27)$$

For the solutions of T_{1p} and T_{2p}

$$T_{1p} = \left| \frac{\alpha_3 q'''}{\rho_1 c_1} + \alpha_1(\alpha_3-\alpha_2)T_f \right| \quad \left|\alpha_1(\alpha_3-\alpha_2)\right| \qquad (B.28)$$

$$T_{2p} = \left| \frac{\alpha_2 q'''}{\rho_1 c_1} + \alpha_1(\alpha_3-\alpha_2)T_f \right| \quad \left|\alpha_1(\alpha_3-\alpha_2)\right| \qquad (B.29)$$

with

$$\beta = \frac{q'''}{\rho_1 c_1 \alpha_1(\alpha_3-\alpha_2)} \qquad (B.30)$$

$$T_{1p} = T_f + \alpha_3\beta \qquad (B.31)$$

$$T_{2p} = T_f + \alpha_2\beta \qquad (B.32)$$

The general solutions of equations (B.8) and (B.14) will be

$$T_1(t) = T_{1H} + T_{1p}$$
$$T_2(t) = T_{2H} + T_{2p} \qquad (B.33)$$

$$T_1(t) = C_1 e^{r_1 t} + C_2 e^{r_2 t} + \alpha_3\beta + T_f \qquad (B.34)$$

$$T_2(t) = d_1 e^{r_1 t} + d_2 e^{r_2 t} + \alpha_2\beta + T_f \qquad (B.35)$$

Here the constants C_1, C_2, d_1 and d_2 must be determined by setting equations (B.8) and (B.14) equal to zero and substituting equations (B.27) into (B.8) and (B.14), so d_1 and d_2 are found as;

$$d_1 = C_1 \frac{(r_1 + \alpha_1)}{\alpha_1} \tag{B.36}$$

$$d_2 = C_2 \frac{(r_2 + \alpha_1)}{\alpha_1} \tag{B.37}$$

With the use equations (B.36) and (B.37) in equation (B.35).

$$T_2(t) = C_1 \frac{(r_1+\alpha_1)}{\alpha_1} e^{r_1 t} + C_2 \frac{(r_2+\alpha_1)}{\alpha_1} e^{r_2 t} + \alpha_2\beta + T_f \tag{B.38}$$

The constants C_1 and C_2 are evaluated from the initial conditions. The initial conditions are

$$\begin{aligned} T_1(0) &= T_{1,0} \\ T_2(0) &= T_{2,0} \end{aligned} \tag{B.39}$$

Using the initial conditions given in (B.39) in equations (B.34) and (B.38) one obtains;

$$C_1 = \frac{r_2+\alpha_1}{r_2-r_1} T_{1,0} - \frac{\alpha_1}{r_2-r_1} T_{2,0} - T_f \frac{r_2}{r_2-r_1} - \frac{\beta}{r_2-r_1}(r_2\alpha_3 + \alpha_1\alpha_3 - \alpha_1\alpha_2) \tag{B.40}$$

$$C_2 = \frac{\alpha_1}{r_2-r_1} T_{2,0} - \frac{r_1+\alpha_1}{r_2-r_1} T_{1,0} + \frac{r_1}{r_2-r_1} T_f + \frac{\beta}{r_2-r_1}(r_1\alpha_3 + \alpha_1\alpha_3 - \alpha_1\alpha_2) \tag{B.41}$$

Equivalent heat transfer parameters h_1 and h_2

To calculate the heat transfered from the fuel to the cladding and from the cladding to the coolant the parameters h_1 and h_2 in equations (2.7), (2.9), (B.8) and (B.14) must be determined. For the calculation of the parameters h_1 and h_2 the form of the steady state temperature distribution is used (Borak)

Equivalent heat transfer coefficient -h_1-

The one-dimensional heat balance equation in the steady state conditions is;

$$q_x A\, dq - q_x A dx - \frac{dq_x}{dx}\, dx\, A + q''' .A dx = 0 \qquad (B.42)$$

$$-\frac{dq_x}{dx} = -q'''$$

Using Fourier's law of conduction

$$-k_1 \frac{d}{dx}\left|\frac{-d\, T_1(x)}{dx}\right| = -q''' \qquad (B.43)$$

$$-k_1 \frac{d^2 T_1(x)}{dx^2} = -q'''$$

$$T_1(x) = -\frac{q'''}{2k_1} x^2 + C_{1x} + C_2 \qquad (B.44)$$

The boundary conditions for equation (B.44) Figure (II-2) are;

$$\frac{dT_1(x)}{dx} = 0 \qquad \text{at} \qquad x = 0$$

$$T_1(x) = T_{12} \qquad \text{at} \qquad x = L_1 \qquad (B.45)$$

Using the boundary conditions given in (B.45) in equation (B.44)

$$C_1 = 0 \tag{B.46}$$

$$C_2 = T_{12} + \frac{q'''}{2k_1} L_1^2 \tag{B.47}$$

The temperature distribution in the fuel for the steady state is found as;

$$T_1(x) = \frac{q'''}{2_{k1}} \left[L_1^2 - X^2\right] + T_{12} \tag{B.48}$$

The steady temperature distribution for the cladding is as follows;

$$k_2 \frac{d^2 T_2(x)}{dx^2} = 0 \tag{B.49}$$

$$T_2(x) = d_1 x + d_2 \tag{B.50}$$

The boundary conditions for equation (B.50) are;

$$T_2(x) = T_{12} \quad \text{at} \quad x = L_1 \tag{B.51}$$

$$-k_1 \frac{dT_1(x)}{dx} = -k_2 \frac{dT_2(x)}{dx} \quad \text{at} \quad x = L_1 \tag{B.52}$$

Using the boundary conditions given in (B.51) and (B.52) the constants d_1 and d_2 are found as below.

$$d_1 = - \frac{q''' \cdot L_1}{k_2} \tag{B.53}$$

$$d_2 = T_{12} + \frac{q''' L_1^2}{k_2} \tag{B.54}$$

$$T_2(x) = \frac{q'''}{k_2} L_1(L_1-x) + T_{12} \qquad (B.55)$$

The heat flux from the fuel to the cladding at $x=L_1$ is given by;

$$-k_1 \frac{dT_1(x)}{dx}\bigg|_{x=L_1} = q'' \qquad (B.56)$$

But in equation (B.4) the heat flux is taken as;

$$q'' = h_1(T_1(t) - T_2(t)) \qquad (B.57)$$

here $T_1(t)$ and $T_2(t)$ are the fuel and cladding temperatures and as time approaches to infinty they will be the mean fuel and mean cladding temperatures $\bar{T}_1$ and $\bar{T}_2$

Hence equations (B.56) and (B.57) are equal and may be written as;

$$h_1 = \frac{-k_1 \left.\frac{dT_1(x)}{dx}\right|_{x=L_1}}{\bar{T}_1 - \bar{T}_2} \qquad (B.58)$$

The mean fuel temperature is calculated from (B.48)

$$\bar{T}_1(x) = \frac{1}{L_1} \int_0^{L_1} \left[\frac{q'''}{2k_1} (L_1^2 - x^2) + T_{12} \right] dx \qquad (B.59)$$

$$= \frac{1}{L_1} \left| \frac{q'''}{2k_1} L_1^2 x - \frac{q'''}{6k_1} x^3 + T_{12} x \right|_0^{L_1}$$

$$\bar{T}_1(x) = T_{12} + \frac{q''' L_1^2}{3k_1} \qquad (B.60)$$

The mean cladding temperature is found from (B.55)

$$\bar{T}_2 = \frac{1}{L_2} \int_{L_1}^{L_2} \left[\frac{q'''}{k_2} L_1(L_1-x) + T_{12} \right] dx \qquad (B.61)$$

$$= T_{12}(L_1+L_2) - T_{12}L_1 + \frac{q'''}{k_2} L_1(L_1+L_2) - \frac{q'''}{k_2} L_1^3$$

$$- \frac{q'''}{2k_2} L_1(L_1 + L_2)^2 + \frac{q'''}{2k_2} L_1^3$$

$$\bar{T}_2 = T_{12} - \frac{q'''}{2k_2} L_1 L_2 \qquad (B.62)$$

Usign equation (B.48) and introducing equations (B.60) and (B.62) into (B.58)

$$h_1 = \frac{q''.L_1}{\frac{q''' L_1^2}{3k_1} + \frac{q''' L_1 . L_2}{2k_2}}$$

$$= \frac{1}{\frac{L_1}{3k_1} + \frac{L_2}{2k_2}} \qquad (B.63)$$

Equivalent heat transfer coefficient $-h_2-$

For the calculation of heat transfered from the cladding to the coolant in equation (B.9) and (2.9) the heat flux is given as

$$q'' = h_2 \left[T_2(t) - T_f \right] \qquad (B.64)$$

as $t \to \infty$, $T_2(t)$ will be the mean cladding temperature $\bar{T}_2$. So, equation (B.64) is equal to the heat transfered from cladding

to the coolant by convection.

From Newton's cooling law the heat transfered by convection at $x = L_1+L_2$ Figure (II-2)

$$h\left[T_2(x=L_1+L_2)-T_f\right] \tag{B.65}$$

From equations (B.64) and (B.65)

$$h_2 = \frac{h\{T_2(x=L_1\ L_2)-T_f\}}{\bar{T}_2 - T_f} \tag{B.66}$$

Using equation (B.50), $\bar{T}_2$ will be;

$$\bar{T}_2 = \frac{1}{L_2}\int_{L_1}^{L_1+L_2} (d_1x + d_2)dx$$

$$\bar{T}_2 = \frac{d_1}{2}(L_2 + 2L_1) + d_2 \tag{B.67}$$

The heat transfered from the cladding to the coolant by conduction is equal to the heat transfered by convection at $x = L_1\ L_2$ (Fig.II-2)

$$q_x = q_c$$

$$-k_2 \left.\frac{dT_2(x)}{dx}\right|_{x=L_1+L_2} = h\left[T_2(x=L_1+L_2) - T_f\right] \tag{B.68}$$

where h is convective heat transfere coefficient

$$-k_2 \left.\frac{dT_2(x)}{dx}\right|_{x=L_1+L_2} = h\ d_1(L_1+L_2)\ d_2 - T_f$$

$$-k_2 \frac{d_1}{h} = d_1(L_1+L_2)\ d_2 - T_f$$

$$h_2 = \frac{h(d_1L_1 + d_1L_2 + d_2 - T_f}{d_1L_1 + d_1L_2 + d_2 - d_1L_2 + \frac{d_1}{2} L_2 - T_f} \qquad (B.69)$$

$$= \frac{-k_2 \frac{d_1}{h} \cdot h}{-k_2 \frac{d_1}{h} - \frac{d_1L_2}{2}}$$

$$= \frac{1}{\frac{1}{h} + \frac{L_2}{2k_2}} \qquad (B.70)$$

APPENDIX C

DERIVATION OF EQUATIONS FOR CONVECTION MODEL OF COBRA III-C

DERIVATION OF EQUATION FOR CONVECTION MODEL USED IN COBRA III-C

The conservation equations of mass, energy, axial momentum, and transverse momentum can be derived in differential form by considering the transport in and out of a control volume consisting of a length dx of subchannel (i) connected to an arbitrary subchannel (j). For the derivation of equations the assumptions given in the general description of the convection model are used together with a few additional assumptions that are required to formulate complete equations.

Figures, C-1, C-2, C-3 show the control volume and the relevant quantities conserved but for clarity only one adjacent subchannel is shown. The conservation equations are obtained directly from the control volume quantities of these figures (Rowe,D.S., Bowring Weisman,J.-75).

The Continuity Equation;

Applying the continuity equation for a control volume to subchannel (i) which is adjacent to subchannel (j). Fig. C-1

Outflow - Inflow + Increase of storage = 0

$$\frac{\partial}{\partial t} \rho_i A_i dx = m_i - (m_i + \frac{\partial m_i}{\partial x} dx) + W'_{jidx} - W'_{ijdx} - W_{ijdx} \qquad (C-1)$$

Where; ρ_i, m_i, A_i, W'_{ji}, W'_{ij}, W_{ij} are density (M/L^3), flow rate (M/T) cross-sectional area (L^2), diversion crossflow from subchannel (j) to subchannel (i), diversion crossflow from subchannel (i) to subchannel (j), turbulent crossflow between adjacent subchannels (Mass/Time.Length) respectively.

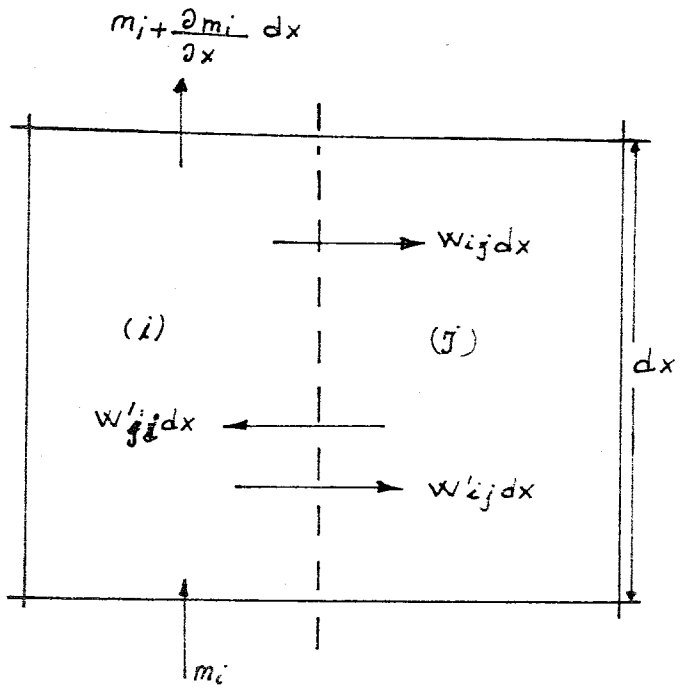

FIGURE C-1- Mass balance (Eq.(C-3) after Ref. (Rowe,D.S.) (BNWL-1965).

Assumptions; 1- Turbulent mixing flow rate are assumed to be equal between adjacent subchannels.

2- The cross-sectional area is constant within time.

Using the assumptions given aboje $W'_{ij} = W'_{ji}$ and $\frac{\partial A_i}{\partial t} = 0$ equation (C-1) reduces to;

$$A_i \frac{\partial \rho_i}{\partial t} + \frac{\partial m_i}{\partial x} = - W_{ij} \qquad (C.2)$$

By considering all adjacent subchannels,

$$A_i \frac{\partial \rho_i}{\partial t} + \frac{\partial m_i}{\partial x} = - \sum_{j=1}^{N} W_{ij} \qquad (C.3)$$

The right side of eq. (C.3) gives the subchannel flow in terms of diversion crossflow. The left side is the time derivative of density gives the component of flow change caused by the fluid expansion.

Energy Conservation Equation;

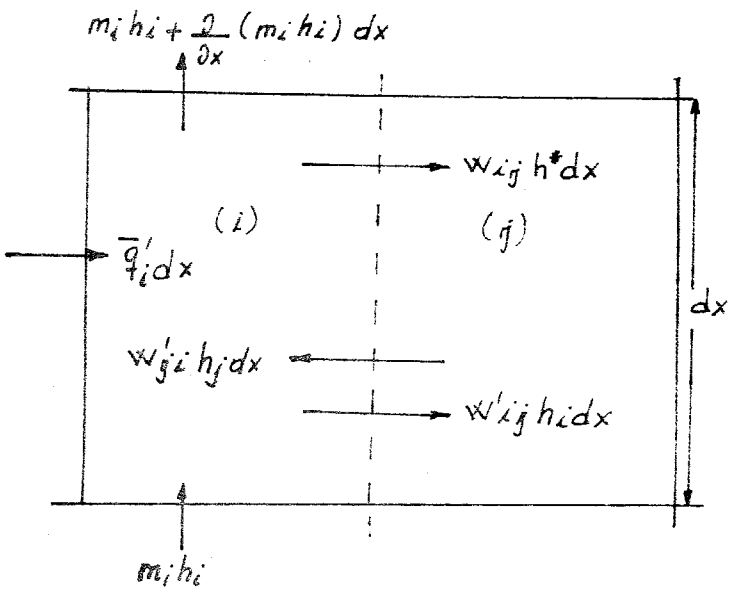

FIGURE C-2- Energy balance (Eq.(C-19) after Ref.(Rowe,D.S.) (BNWL-1695).

Consider the energy that might cross the control surface and the change of energy storage that might take place within the control volume. Applying the energy conservation for the control volume to subchannel (i) which is adjacent to subchannel (j) (Holman,J.P., Kays,W.M.) the rate of change of the total energy in the control volume will be;

$$\frac{\partial}{\partial t} \rho_i'' U_i A_i dx = m_i h_i - (m_i h_i + \frac{\partial}{\partial x} m_i h_i dx) + W_{ji}' h_j dx - W_{ij}' h_i dx$$

$$- W_{ij} h \, dx + \bar{q}_i' dx \qquad (C.4)$$

Where; ρ_i'', U_i, A_i, m_i, W_{ji}', W_{ij}, h , $\bar{q}_i'$ are the effective density for enthalpy transport (M/L^3), internal energy (H/M), cross-sectional area (L^2), flow rate (MIT), turbulent cross-flow between adjacent subchannels (M/TL), diversion crossflow between adjacent subchannels (M/TL), enthalpy carried by diversion crossflow (H/M), and heat addition per unit length (H/TL) and the subscrips (i) and (j) denote the subchannel identification numbers. The dimensions L, T, M, H, L^2 denote length in (ft), time in (hours or sec), mass in (lbm), energy in (Btu), length square in (ft^2) respectively.

In eq.(C.4) the internal energy-u- is obtained from;

$$h = u + pv$$

$$V = \frac{1}{\rho} \qquad \text{for all unit mass} \qquad (C.5)$$

from eq.(C.5)

$$U = h - P/\rho \qquad \text{and} \qquad \rho u = \rho h - p \qquad (C.6)$$

substituting eq. (C.6) into eq. (C.4) and assuming that:

1- The cross-sectional area is constant within the time.

2- Turbulent mixing flowrate is assumed to be equal between each adjacent subchannels.

3- Sonic velocity progagation is omitted.

$$A_i \frac{\partial}{\partial t} (\rho_i'' h_i - p) + \frac{\partial}{\partial x} m_i h_i = \bar{q}_i' + (h_j - h_i) W_{ij}' - W_{ijh} \qquad (C.7)$$

Where p is the pressure

$$A_i \frac{\partial}{\partial t} \rho_i'' h_i - A_i \frac{\partial P}{\partial t} + \frac{\partial}{\partial x} m_i h_i = \bar{q}_i' + (h_j - h_i) w_{ij}' - W_{ij} h^* \qquad (C.8)$$

neglecting $\partial p/\partial t$ and with the use of the continuity equation given in eq.(C.3).

$$A_i \frac{\partial}{\partial t} (\rho_i'' h_i) + m_i \frac{\partial h_i}{\partial x} + h_i(-W_{ij} - A_i \frac{\partial \rho_i}{\partial t}) = \bar{q}_i' + (h_j - h_i) W_{ij}' - W_{ij} h^* \qquad (C.9)$$

$$A_i (\frac{\partial}{\partial t} \rho_i'' h_i - h_i \frac{\partial \rho_i}{\partial t}) + m_i \frac{\partial h_i}{\partial x} = \bar{q}_i' + (h_j - h_i) W_{ij}' + (h_i - h^*) W_{ij} \qquad (C.10)$$

dividing eq.(C.10) by m_i

$$\frac{A_i}{m_i} (\frac{\partial}{\partial t} \rho_i'' h_i - h_i \frac{\partial \rho_i}{\partial t}) + \frac{\partial h_i}{\partial x} = \frac{\bar{q}_i'}{m_i} + (h_j - h_i) \frac{W_{ij}'}{m_i} \quad (h_i - h^*) \frac{W_{ij}}{m_i} \qquad (C.11)$$

Where ρ_i'' is the effective density for enthalpy transport and is defined by

$$\rho_i'' = \rho_i - hgf \frac{\partial \psi}{\partial h_i} \qquad (C.12)$$

Where ψ is the slip correction function for energy transport (Tong) and hgf is the latent heat of evaporation (Btu/lb). From eq.(C.11) and (C.12)

$$\frac{A_i}{m_i}\left|h_i\frac{\partial}{\partial t}\left(\rho_i - hgf\frac{\partial\psi}{\partial h_i}\right) + \frac{\partial h_i}{\partial t}\left(\rho_i - hgf\frac{\partial\psi}{\partial h_i}\right) - h_i\frac{\partial\rho_i}{\partial t}\right| + \frac{\partial h_i}{\partial x}$$

$$= \frac{\bar{q}_i'}{m_i} + (h_j - h_i)\frac{W'_{ij}}{m_i} + (h_i - h^*)\frac{W_{ij}}{m_i} \qquad (C.13)$$

$$\frac{A_i}{m_i}\left|h_i\frac{\partial\rho_i}{\partial t} - h_i\frac{\partial}{\partial t}(hgf\,\partial\psi/\partial t) + \frac{\partial h_i}{\partial t}\left(\rho_i - hgf\frac{\partial\psi}{\partial}\right) - h_i\frac{\partial\rho_i}{\partial t}\right| + \frac{\partial h_i}{\partial x}$$

$$= \frac{\bar{q}_i'}{m_i} + (h_j - h_i)\frac{W_{ij}}{m_i} + (h_i - h^*)\frac{W_{ij}}{m_i} \qquad (C.14)$$

$$\frac{A_i}{m_i}\frac{\partial h_i}{\partial t}\left(\rho_i - hgf\frac{\partial\psi}{\partial t}\right) + \frac{\partial h_i}{\partial x} = \frac{\bar{q}_i'}{m_i} + (h_j - h_i)\frac{W'_{ij}}{m_i} + (h_i - h^*)\frac{W_{ij}}{m_i} \qquad (C.15)$$

Where;

$$\frac{m_i}{A_i\left(\rho_i - hgf\frac{\partial\psi}{\partial h_i}\right)} = U'' \qquad (C.16)$$

U'' is the effective enthalpy thermal velocity.

Substituting eq. (C.16) into eq. (C.15)

$$\frac{1}{U''_i}\cdot\frac{\partial h_i}{\partial t} + \frac{\partial h_i}{\partial x} = \frac{\bar{q}_i'}{m_i} + (h_j - h_i)\frac{W_{ij}}{m_i} + (h_i - h^*)\frac{W_{ij}}{m_i} \qquad (C.17)$$

The heat transfer term in eq.(C.17) includes two terms. One of these terms is the heat transfer rate from the fuel surface and the other term is the thermal conduction between adjacent subchannels.

The heat transfer rate from the fuel surface to the fluid depends on the fuel surface temperature, fluid temperature and surface heat transfer coefficient. The thermal conduction between adjacent subchannels is assumed to be proportional to the subchannel temperature differences and depends on the subchannel geometry and fluid thermal conductivity.

The thermal conduction term $\bar{q}_i'$ is given by.

$$\bar{q}_i' = q_i + (t_j - t_i)\, C_{ij} \qquad (C.18)$$

Where c_{ij} is the thermal conduction coefficient.

With the use of eq.(C.18) and considering all adjacent subchannels the energy conservation equation takes the form;

$$\frac{1}{U_i''}\frac{\partial h_i}{\partial t} + \frac{\partial h_i}{\partial x} = \frac{\bar{q}_i'}{m_i} - \sum_{j=1}^{N} (t_i - t_j)\frac{c_{ij}}{m_i} - \sum_{j=1}^{N} (h_i - h_j)\frac{W_{ij}}{m_i} +$$

$$\sum_{j=1}^{N} (h_i - h^*)\frac{W_{ij}}{m_i} \qquad (C.19)$$

The terms on the left side of eq.(C.19) give the rate of transient and spatial change of enthalpy. The first term depends on the effective transport velocity which is related to the time durating of the transient. The first term on the right side gives the rate of enthalpy change, the second term accounts for the conduction mixing. The third term gives the turbulent enthalpy transport between all interconnected subchannels and the fourth term gives the energy carried by diversion crossflow.

Axial Momentum Equation;

The momentum of an element may be defined as a quantity proportional to the product of the mass of that element and its velocity.

The momentum theorem applied to the control volume will be outflow minus inflow plus increase of storage is equal all external forces acting to the control volume.

Applying the momentum equation to the control volume shogn in Fig.C-3 one obtains

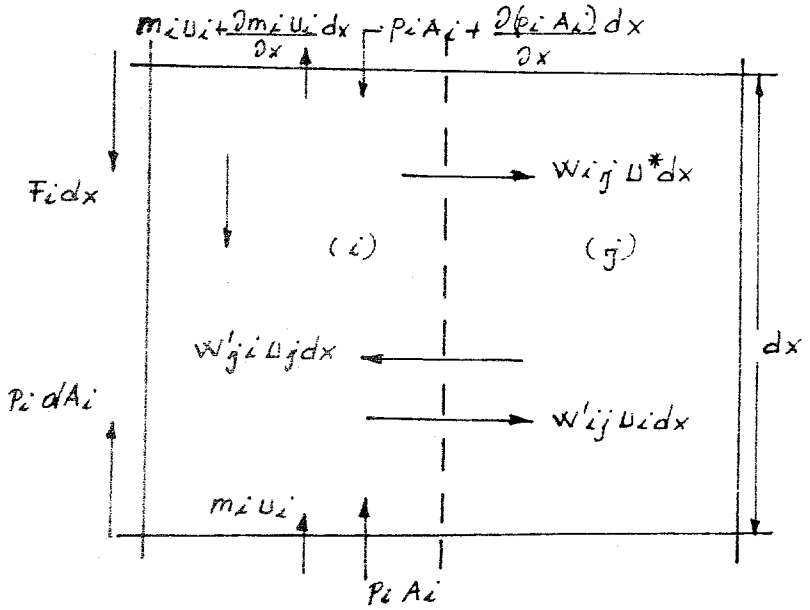

FIGURE C-3; Axial Momentum Balance Eq.(C-30) after Ref. (Rowe.D.S.) (BNWL-1695)

$$\frac{\partial m_i}{\partial t} dx = -F_i dx - A_i g \rho_i \cos\Theta dx + p_i dA_i + m_i u_i + m_i u_i -$$

$$-(m_i u_i + \frac{\partial}{\partial x} m_i u_i dx) + p_i A_i - (p_i A_i + \frac{\partial}{\partial x} p_i A_i dx)$$

$$+ W'_{ji} u_j dx - W'_{ij} u_i dx - W_{ij} u^* dx \qquad (C.20)$$

Assume; 1- The cross-sectional area is constant.

2- Turbulent crossflow is equal between adjacent subchannels.

$$\frac{\partial}{\partial t} m_i = -F_i - A_i g \rho_i \cos\theta - \frac{\partial}{\partial x}(m_i u_i) - A_i \frac{\partial p_i}{\partial x} + (u_j - u_i) W'_{ij} - W_{ij} u^* \quad (C.21)$$

where; m_i, F_i, u_i, p, W, W', g, ρ, u are mass flow rate (M/T) the friction force loses (M/LT^2), effective momentum velocity (L/T), pressure (F/L^2), effective momentum velocity (L/T), pressure (F/L^2), diversion crossflow between adjecent subchannels (M/TL), turbulent crossflow between adjacent subchannels (M/TL), gravitational constant (L/T^2), density (M/L^3), and effective velocity carried by diversion crossflow (L/T) respectively.

For the loss term the following relation is used (Tong,L.S.)

$$F_i = \left| \frac{A_i V'_i f_i \phi_i}{2D_i} + \frac{A_i K_i V'_i}{2\Delta x} \right| \left| \frac{m_i}{A_i} \right|^2 \quad (C.22)$$

where; f_i, V'_i, ϕ_i, k_i, A_i, D_i are friction factor effective specific momentum volume, two phase friction multiplier, spacer loss coefficient, cross-sectional area, diameter.

The first term of eq.(C.22) presents the skin friction loss per length, the second term accounts for the spacer loses.

Using eq.(C.22) and the continuity equation (C.3) eq. (C.21) will be;

$$-\left| \frac{A_i f_i V'_i \phi_i}{2D_i} + \frac{K_i V'_i A_i}{2\Delta x} \right| \left| \frac{m_i}{A_i} \right|^2 - A_i g \rho_i \cos\theta - u_i \left(-W_{ij} - A_i \frac{\partial \rho_i}{\partial t}\right)$$

$$- m_i\left(\frac{\partial u_i}{\partial x}\right) - A_i \frac{\partial p_i}{\partial x} = \frac{\partial m_i}{\partial t} + (u_i - u_j)W'_{ij} + u^*W_{ij} \qquad (C.23)$$

Defining the momentum velocity u_i in terms of specific momentum volume, flow rate, and area,

$$u_i = \frac{m_i V'_i}{A_i} \qquad (C.24)$$

Introducing eq.(C.24) into eq.(C.23)

$$-\left| \frac{A_i f_i V'_i \phi_i}{2D_i} + \frac{K_i V'_i A_i}{2x} \right| \left| \frac{m_i}{A_i} \right|^2 - A_i g \rho_i \cos\theta + u_i W_{ij}$$

$$+ A_i u_i \frac{\partial \rho_i}{\partial t} - \frac{m_i}{A_i}\left(V'_i \frac{\partial m_i}{\partial x} + m_i \frac{\partial V'_i}{\partial x}\right) - A_i \frac{\partial p_i}{\partial x} = \frac{\partial m_i}{\partial t}$$

$$+ (u_i - u_j)W'_{ij} + u^*W_{ij} \qquad (C.25)$$

$$-\left| \frac{A_i f_i V'_i \phi_i}{2D_i} + \frac{K_i V'_i A_i}{2x} \right| \left| \frac{m_i}{A_i} \right|^2 - A_i g \rho_i \cos\theta + u_1 W'_{ij}$$

$$A_i u_i \frac{\partial \rho_i}{\partial t} - \frac{m_i V'_i}{A_i} \frac{\partial m_i}{\partial x} - \frac{m_i^2}{A_i} \frac{\partial V'_i}{\partial x} - A_i \frac{\partial p_i}{\partial x} = \frac{\partial m_i}{\partial t}$$

$$+ (u_i - u_j)W'_{ij} + u^*W_{ij} \qquad (C.26)$$

Where; $\frac{\partial m_i}{\partial x} = - W_{ij} - A_i \frac{\partial \rho_i}{\partial t}$

and

$$\frac{m_i V'_i}{A_i} = u_i$$

$$-\left| \frac{A_i f_i V'_i \phi_i}{2D_i} + \frac{K_i V'_i A_i}{2x} \right| \left| \frac{m_i}{A_i} \right|^2 - A_i g \rho_i \cos\theta + u_i W'_{ij}$$

$$A_i u_i \frac{\partial \rho_i}{\partial t} - u_i(-W_{ij} - A_i \frac{\partial \rho_i}{\partial t}) - \frac{m_i^2}{x} \frac{\partial v_i}{\partial x} - A_i \frac{\partial p_i}{\partial x} =$$

$$\frac{\partial m_i}{\partial t} + (u_i - u_j)W'_{ij} + u^* W_{ij} \qquad (C.27)$$

$$-\left|\frac{A_i f_i V'_i \phi_i}{2D_i} + \frac{K_i V'_i A_i}{2x}\right| \left|\frac{m_i}{A_i}\right|^2 - A_i g \rho_i \cos + 2u_i W_{ij}$$

$$2A_i u_i \frac{\partial \rho_i}{\partial t} - \frac{m_i^2}{A_i} \frac{\partial v'_i}{\partial x} - A_i \frac{\partial p_i}{\partial t} = \frac{\partial m_i}{\partial t} \quad (u_i - u_i)W'_{ij} \quad u W_{ij} \qquad (C.28)$$

Dividing eq.(C.28) by A_i and rearranging we obtain

$$\frac{1}{A_i} \frac{\partial m_i}{\partial t} - 2u_i \frac{\partial \rho_i}{\partial t} + \frac{\partial p_i}{\partial x} = -\left|\frac{f_i V'_i \phi_1}{2D_i} \quad \frac{K_i V'_i}{2\Delta x} + \frac{\partial V'_i}{\partial x}\right| \left|\frac{m_i}{A_i}\right|^2$$

$$-(u_i - u_j) \frac{W'_{ij}}{A_i} + (2u_i - u_i^*) \frac{W_{ij}}{A_i} - g\rho_i \cos\theta \qquad (C.29)$$

There exists an eddy diffusion of heat and momentum due to the turbulent crossflow. Therefore the turbulent mixing crossflow term is multiplied by the turbulent factor $-f_T-$.

By considering all adjacent subchannels and including the turbulent momentum factor, the axial momentum balance equation takes the form as;

$$\frac{1}{A_i} \frac{\partial m_i}{\partial t} - 2u_i \frac{\partial \rho_i}{\partial t} + \frac{\partial p_i}{\partial x} = -\left|\frac{m_i}{A_i}\right|^2 \left|\frac{V'_i f_i \phi_i}{2D_i} + \frac{K_i V'_i}{2\Delta x} + \frac{\partial V'_i}{\partial x}\right|$$

$$-g\rho_i \cos\theta - f_T \sum_{j=1}^{N} (u_i - u_j) \frac{W'_{ij}}{A_i} + \sum_{j=1}^{N} (2u_i - u^*) \frac{W_{ij}}{A_i} \qquad (C.30)$$

The terms on the left side of the axial momentum balance equation (C.30) are the transient component of the axial pressure gradient and the spatial rate of change of the pressure. The right side gives the frictional, spatial, acceleration and elavation components of the pressure gradient. The fifth term accounts for the turbulent crossflow and equalize the velocities of adjacent subchannels. The sixth term is the diversion crossflow term, gives the momentum changes due to velocity changes in the subchannels.

Transverse Momentum Equation;

Fig.(C-4) shows a rectangular control volume placed in the gap between two subchannels.

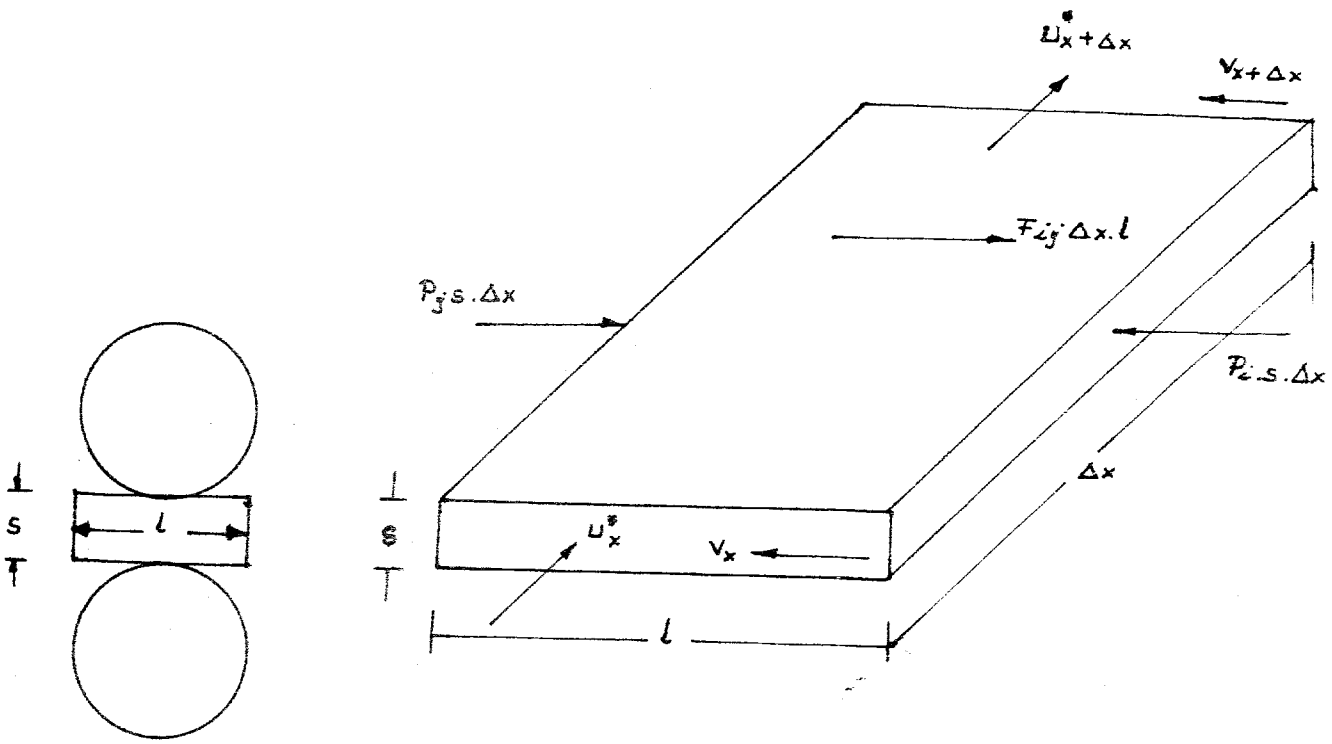

FIGURE C-4 Control volume for Transverse Momentum Balance (Eq.(C-36) after Ref.(Rowe.D.S. BNWL-1695).

By the formulation of the transverse momentum balance equation it is assumed that the difference between crossflow momentum flux entering and leaving the control volume through the transverse surfaces is negligibly small.

Applying the conservation of momentum equation to the control volume in the transverse direction (Fig.C-4) gives;

$$-F_{ij}\Delta x l - P_j s\Delta x + P_i s\Delta x + (\rho^* s l u^* v)_x - (\rho^* s l u^* v)_{x+\Delta x} = \frac{\partial \rho^*}{\partial t} s l \Delta x v \quad (C.31)$$

Where; v, u^*, p, ρ^*, s, l, are the transverse velocity, effective velocity carried by diversion crossflow, pressure, density of diversion crossflow, rod spacing, gap length and F_{ij} represents the friction and form pressure loss due to crossflow.

The first term in Eq.(C-31) represents the friction losses, the second and third termson the left side are the force terms existing due to the net pressure differences.

$(\rho^* s l u^* v)x$ denotes the enterence of the transverse momentum through the transverse surface.

$(\rho^* l u^* v)_{x+\Delta x}$ represents the momentum leaving out of the transverse control volume. The right side of Eq.(C.31) gives the rate of change of the transverse momentum.

Dividing Eq.(C.31) by Δx gives;

$$- F_i j l - P_j s + P_i s = \frac{\partial \rho^*}{\partial t} s l v + \frac{(\rho^* s l u^* v)_{x+\Delta x} - (\rho^* s l u^* v)x}{\Delta x} \quad (C.32)$$

It is assumed that Δx is sufficiently small. Hence taking limit as Δx goes to zero;

$$\frac{\partial(\rho^* slu^* v)}{\partial x} = \left| \frac{(\rho^* slu^* v)_{x+\Delta x} - (\rho^* slu^* v)_x}{\partial x} \right| \qquad (C.33)$$

Where; $\rho^* sv = W_{ij}$ (C.34)

$$\frac{(W_{ij} lu^*)}{\partial x} = \frac{(W_i jlu^*)_{x+\Delta x} - (W_i jlu^*)_x}{\Delta x} \qquad (C.35)$$

Dividing Eq.(C.32) by l and introducing Eq.(C.35) into Eq.(C.32)

$$-F_{ij} + (p_i - p_j)\frac{s}{l} = \frac{\partial W_{ij}}{\partial x} + \frac{\partial W_{ij} \cdot u^*}{\partial x} \qquad (C.36)$$

Eq.(C.36) accounts for the transverse momentum balance existing in the presence of blockages around the bundle area due to the effect of crossflow.

F_{ij} in Eq.(C.36) is the friction and form the pressure loss due to crossflow for steady flow, setting the right hand side of Eq.(C.36) to zero one obtains;

$$-F_{ij} + (p_i - p_j)\frac{s}{l} = 0 \qquad (C.37)$$

Where

$$P_i - P_j = \frac{K\rho^* v^2}{2} \qquad (C.38)$$

K is the cross flow resistance factor and given as input. Substituiting Eq.(C.38) into Eq.(C.37)

$$\frac{s}{l}\frac{k\rho^* v^2}{2} = F_{ij} \qquad (C.39)$$

Eq.(C.39) is multiplied and divided by $\rho.s^2$ and introducing Eq.(C.34) into Eq.(C.39) F_{ij} is found as.

$$F_{ij} = \left(\frac{s}{l}\right) \cdot \frac{K|W|W}{2s^2\rho^*} \qquad (C.40)$$

In Eq (C.40) K includes both the friction and the loss components of the transverse pressure drop and given as input, as cross-flow resistance factor. Equation (C.40) will be

$$F_{ij} = C_{ij} W_{ij} \left(\frac{s}{l}\right) \qquad (C.41)$$

Where;

$$C = \frac{K|W|}{2s^2\rho^*} \qquad (C.42)$$

Substituiting Eq.(C.41) into (C.36), the transverse momentum balance equation takes the form as;

$$\frac{\partial W_{ij}}{\partial t} + \frac{\partial(u^*_{ij} W_{ij})}{\partial x} + \left(\frac{s}{l}\right) C_{ij} W_{ij} = \left(\frac{s}{l}\right) (p_i - p_j) \qquad (C.43)$$

APPENDIX D

DERIVATION OF EQUATIONS FOR CONVECTION MODEL OF TERHID

DERIVATION OF EQUATIONS FOR CONVECTION MODEL USED IN TERHID

The equations contained in the convection model of TERHID are derived by using the differential form and considerind the transport in and out a control volume consisting of a length dz., with the required assumptions. Figures (D-1), (D-2), (D-3) show the control volumes and the relavent conserved quantities.

The Continuity Equation:

Consider the mass rate of flow across the control surface and the rate of change of mass storage within the control volume for a cross-sectional area and length dz as shown in Fig.(D-1) below;

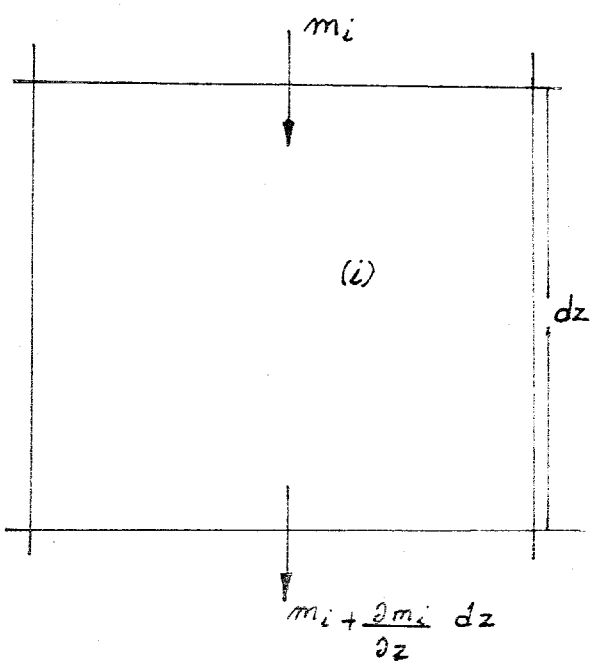

FIGURE (D-1) Mass Balance |Eq(D.2) after. Ref. (Borak,F.)(TERHID)|.

Change of mass storage = Inflow-Outflow

$$\frac{\partial \rho_i}{\partial t} A_i d_z = m_i - (m_i + \frac{\partial m_i}{\partial z} dz) \qquad (D.1)$$

where; A_i, m_i, ρ_i, are the cross-sectional flow area.(m^2), flow rate (kg/sec), density of the fluid (kg/m^3).

Assume; the cross-sectional area is constant within time.

$$A_i \frac{\partial \rho_i}{\partial t} \quad \frac{\partial m_i}{\partial z} = 0 \qquad (D.2)$$

Eq.(D.2) is the continuity equation gives the component of flow change by fluid expansion.

Energy Conservation Equation;

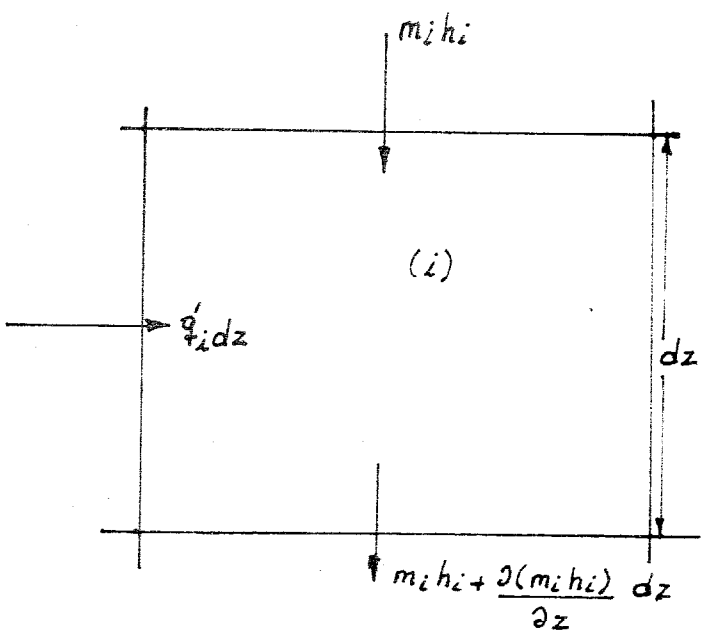

Figure.(D-2). Energy Balance |Eq.(D.10) after Ref.(Borak,F.)(TERHID

The application of the principle of conservation of energy to energy to the Control volume shown in Figure (D-2) yields;

$$\frac{\partial}{\partial t}(\rho_i U_i A_i)\,dz = m_i h_i - (m_i h_i + \frac{\partial m_i h_i}{\partial z}\,dz) + q_i'\,dz. \qquad (D.3)$$

Where; $\rho_i, U_i, A_i, m_i, h_i, q_i'$ are fluid density (kg/m^3), internal energy of the coolant (J/kg), the cross-sectional flow area (m^2) flow rate (kg/sn), enthalpy of the coolant (J/kg), heat addition per unit length from the fuel to the coolant (W/m), respectively. The internal energy u_i is defined as;

$$U_i = h_i - P_i v_i \quad \text{and} \quad v_i = \frac{1}{\rho_i} \text{ for all unit mass} \qquad (D.4)$$

$$U_i = h_i - \frac{P_i}{\rho_i} \qquad (D.5)$$

With the use of eq.(D.5) in eq.(D.3) and assuming that the cross-sectional area is constant within time eq.(D.3) yields

$$A_i \frac{\partial}{\partial t}(\rho_i h_i - P_i) = \frac{\partial (m_i h_i)}{\partial z} + q_i' \qquad (D.6)$$

Using the continuity equation given in (D.2)

$$\frac{\partial m_i}{\partial z} = -A_i \frac{\partial \rho_i}{\partial t} \qquad (D.2) \qquad (D.2$$

$$A_i \rho_i \frac{\partial h_i}{\partial t} - A_i \frac{\partial p_i}{\partial t} = - m_i \frac{\partial h_i}{\partial z} + q_i' \qquad (D.7)$$

By assuming $\frac{\partial p_i}{t} = 0$

and dividing eq.(D.7) by m_i

$$\frac{A_i \rho_i}{m_i} \frac{\partial h_i}{\partial t} + \frac{\partial h_i}{\partial z} = \frac{q_i'}{m_i} \qquad (D.8)$$

With the definition of the velocity carried by the coolant

$$V_i = \frac{m_i}{A_i \rho_i} \tag{D.9}$$

$$\frac{1}{V_i}\frac{\partial h_i}{\partial t} \quad \frac{\partial h_i}{\partial z} = \frac{q_i'}{m_i} \tag{D.10}$$

Eq.(D.10) accounts for the energy balance in the coolant flow channel. The terms on the left hand side calculate the transient and spatial change of enthalpy. The transient change of enthalpy depends on the fluid transport velocity during the time of the transients.

The Momentum Equation:

The momentum theorem when applied to the control volume (i) as in Fig (D-3) may be expressed as;

Change of Momentum Storage = Inflow - outflow + all external forces acting on the control volume or surface.

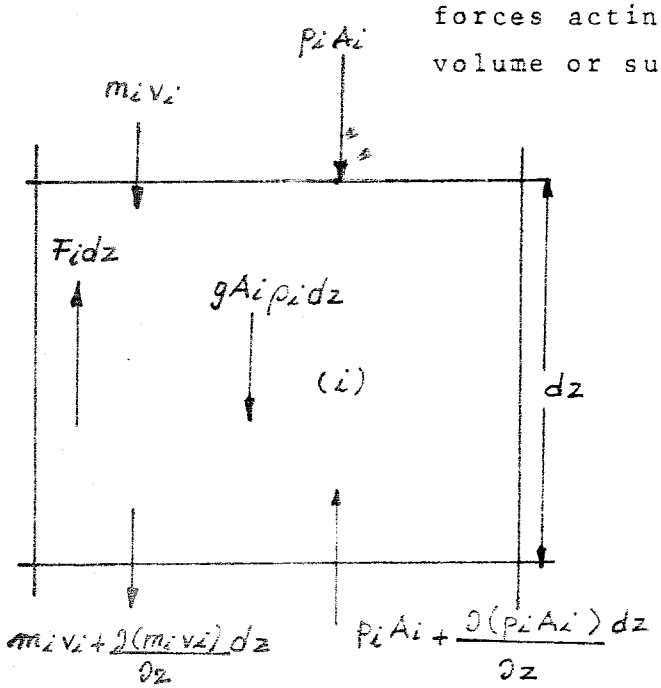

FIGURE(D-3) Momentum Balance |Eq.(D.16) after Ref.(Borak.F)(TERHID)|

$$\frac{\partial m_i}{\partial t} dz = m_i v_i - \left(m_i v_i \quad \frac{\partial (m_i v_i)}{\partial z} dz\right) + p_i A_i - \left(p_i A_i + \frac{\partial (p_i A_i)}{\partial z} dz\right)$$

$$+ g A_i \rho_i dz - F_i dz \qquad (D.11)$$

Where; F_i, v_i, g, are the frictional losses per unit length (N/m), velocity of the fluid (m/sec) and the gravitational accelaration, respectively.

By assuming that the cross-sectional flow area is constant, Eq.(D-11) simplyfies to

$$\frac{\partial m_i}{\partial t} = - \frac{\partial (m_i v_i)}{\partial z} - A_i \frac{\partial p_i}{\partial z} + g A_i \rho_i - F_i \qquad (D.12)$$

With the definition of the flow velocity - vi - eq.(D.9) eq.(D.12) takes the form,

$$\frac{\partial m_i}{\partial t} = - \frac{1}{A_i} \frac{\partial (m_i^2 / \rho i)}{\partial z} - A_i \frac{\partial p_i}{\partial z} + g A_i \rho_i - F_i \qquad (D.13)$$

$$\frac{\partial m_i}{\partial t} = - \frac{2 m_i}{\rho_i A_i} \frac{\partial m_i}{\partial z} + \frac{m_i^2}{A_i} \frac{\partial (1/\rho_i)}{\partial z} - A_i \frac{\partial p_i}{\partial z} + g A_i \rho_i - F_i \qquad (D.14)$$

Dividing eq.(D.14) by A_i and using eq.(D.9)

$$\frac{1}{A_i} \frac{\partial m_i}{\partial t} = - \frac{2 v_i}{A_i} \frac{\partial m_i}{\partial z} + \left|\frac{m_i}{A_i}\right|^2 \frac{\partial (1/\rho_1)}{\partial z} - \frac{\partial p_i}{\partial z} + g \rho_i - \frac{F_i}{A_i} \qquad (D.15)$$

Using the continuity equation given in eq.(D.2) and rearranging eq.(D.15) yields;

$$\frac{\partial p_i}{\partial z} = g\rho_i + 2v_i \frac{\partial \rho_i}{\partial t} + \left|\frac{m_i}{A_i}\right|^2 \frac{\partial (1/\rho_i)}{\partial z} - \frac{F_i}{A_i} - \frac{1}{A_i} \frac{\partial m_i}{\partial t} \qquad (D.16)$$

Eq.(D.16) accounts for the spatial rate of change of the pressure, the right side of the momentum balance equation includes the elevational, transient, and frictional components of the pressure gradient.

APPENDIX E

LIST OF SUBPROGRAMMES IN COBRA III-C AND TERHID

The subroutines and functions in COBRA-III-C and TERHID are listed below in alphabetical order where the column headings mean:

TYPE : S = Subroutine, F = Function
FROM : Calling Subroutine
CALLS: Called Subroutine or Function

SUBROUTINES AND FUNCTIONS IN COBRA III-C

N A M E	TYPE	P U R P O S E	F R O M	CALLS
HCOOL	F	Surface heat transfer coefficient	HEAT	---
HPROP	F	Liquid specific heat, liquid viscosity, liquid conductivity	PROP	---
HSL	F	Liquid saturation enthalpy	PROP	---
HVAP	F	Vapour enthalpy	PROP	---
MAIN	-	Input data, Control, Output	-	CHF CURVE HSL PROP TSL SCHEME SPLIT
MIX	S	Mixing Equation	SCHEME	CURVE
PROP	S	Fluid Properties	MAIN SCHEME SPLIT	CURVE FMU HPROP HSL HVAP ROLIQ ROVAP SAP SATTEM SURTEN TSL
ROLIQ	F	Liquid Density	PROP	---
ROVAP	F	Vapour Density	PROP	---
S	F	S = -1, 0, 1 Matrix Transformation According to Boundary	DIFFER DIVERT	---

N A M E	TYPE	P U R P O S E	F R O M	CALLS
AREA	S	Variable subchannel area	SCHEME	CURVE
BVOID	F	Void fraction from quatily	VOID	---
CHF	S	Critical heat flux prediction	MAIN	CHF1 CHF2
CHF1	F	B W2 CHF Correlation	CHF	---
CHF2	F	W-3 CHF Correlation	CHF	---
CIJ	F	C_{ij} in transverse Momentum	DIVERT	---
CURVE	S	Linear interpolation between points	AREA HEAT MAIN MIX PROP	---
DECOMP	S	Solves simultanous equations	DIVERT	---
DIFFER	S	Calculates, enthalpy, mass, and pressure	SCHEME SPLIT	S
DIVERT	S	Calculate cross-flow $W_{i,j}$	SCHEME	CIJ DECOMP S SOLVE
FMU	F	Two phase friction multiplier	PROP	---
FORCE	S	Wrap cross-flow	SCHEME	---
GAUSS	S	Solves Temp. by Gauss Elimination	TEMP	---
HEAT	S	Subchannel heat flux	SCHEME	CURVE TEMP HCOOL

N A M E	TYPE	P U R P O S E	F R O M	CALLS
SATTEM	F	Saturation Temperature	PROP	---
SAP	F	Saturation Pressure	PROP	---
SCHEME	S	Main Axial Do LOOP	MAIN	AREA DIFFER DIVERT FORCE HEAT MIX PROP VOID
SQUAL	F	Levy Subcooled Void	VOID	---
SOLVE	S	Solve Simultanous Equa. for cross-flow	DIVERT	---
SPLIT	S	Inlet Flow	MAIN	DIFFER PROP VOID
SURTEN	F	Surface Tension	PROP	---
TEMP	S	Fuel Temperature	HEAT	GAUSS
TSL	F	Liquid Temperature	PROP	---
VOID	S	Void, Density	SCHEME SPLIT	BVOID SQUAL

SUBROUTINES AND FUNCTIONS IN TERHID

N A M E	TYPE	P U R P O S E	F R O M	CALLS
ANA PROGRAM	-	Input, Control, Output	-	CIZIM PLAK TEMP
CIZIM	S	Linear Interpolation between Points	ANA PROGRAM HACGUÇ	---
CPYKT	S	Fuel Specific Heat	TEMP	---
CPZRF	S	Clad. Spesific Heat	TEMP	---
DELTF	S	Coolant Temp. Pressure Losses	TEMP	ISIAKI RHOSU SURTNM TSU
ENTSU	F	Liquid Enthalpy	TEMP	---
HACGUC	S	Power Generation	TEMP	CIZIM
HHSP	S	Convective Heat Transfer Correlation	HZHSP	VISKSU SLETSU OZISI
H1HSP	S	Equivalent Heat Transfer Coefficient $-h_1-$	TEMP	---
H2HSP	S	Equivalent Heat Transfer Coefficient $-h_2-$	TEMP	HHSP
ISIAKI	S	Power transfered from cladding to coolant	DELF	TSU
OZISI	F	Fluid specific Heat	HHSP	---

N A M E	TYPE	P U R P O S E	F R O M	CALLS
PLAK	S	Power Generation At Each Plate	ANA PROGRAM	---
RHOSU	F	Liquid Density	DELP	---
ROYKT	S	Fuel Density	TEMP	---
ROZRF	S	Cladding Density	TEMP	---
SLETSU	F	Liquid Heat Transfer Coefficient	HHSP	---
SURTM	S	Friction factor f_f and Frictional Losses	DELTF	---
TEMP	S	Fuel Temperature Cladd Temperature Fluid Temperature	ANA PROGRAM	CPYKT CPZRF DELTF ENTSU HACGUC H1HSP H2HSP ROYKT DOZRF
TSU	F	Fluid Temp as a function of Enthalpy	DELTF	---
VISKSU	F	Liquid viscosity	HHSP	---